Measurement of W Boson Branching Fractions at 13 TeV with CMS (SMP-18-011)

Ziheng Chen, **Nathaniel Odell**, Mayda Velasco

Norhtwestern University

May 6, 2021

W branching fractions and lepton flavor universality

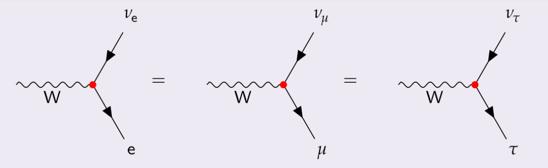

- One of the fundamental assumptions in the SM is that the coupling strength g is the same for all three generations of leptons, $g_e = g_\mu = g_\tau \equiv g_\ell$, known as Lepton Flavor Universality (LFU) in the weak interaction,

$$i\bar{\psi}\not{\partial}\psi = \bar{\chi}_L\gamma^\mu(i\partial_\mu - g\frac{\tau_a}{2}W^a_\mu - g'\frac{Y}{2}B_\mu)\chi_L + \bar{\psi}_R\gamma^\mu(i\partial_\mu - g'\frac{Y}{2}B_\mu)\psi_R - g_s(\bar{q}\gamma^\mu T_a q)G^a_\mu.$$

- Tests of the SM LFU can be performed by studying the leptonic decays of W bosons where the only difference should be from the decay phase space due to different fermion masses.
- In high-energy regime, measurements have been performed at colliders:
  - SPS and Tevatron: $p\bar{p} \to W$;
  - LEP: $e\bar{e} \to WW$;
  - LHC: $pp \to W$ and $pp \to t\bar{t} \to WbWb$.
- In low-energy regime, some of the most stringent LFU tests come from the charged weak decays of mesons (e.g. D, B) and leptonic decays of taus [1]. While most experiments show high precision agreement with LFU, some tension has been observed in the semileptonic decays of B mesons by Belle [2, 3, 4], BaBar [5, 6] and LHCb [7, 8, 9].

SPS and Tevatron

- Measured $\sigma_{p\bar{p}\to W} \times \mathcal{B}(W \to e\nu, \mu\nu, \tau\nu)$.
  - UA1 [10],
  - UA2 [11, 12, 13],
  - CDF [14, 15, 16],
  - D0 [17, 18, 19, 20].
- τ leptons reconstructed in the hadronic decay modes.
- Combined average $g_\tau^W / g_e^W = 0.988 \pm 0.025$ (by D0 [20]) was consistent with SM.

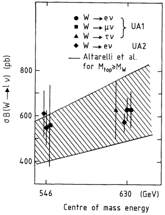

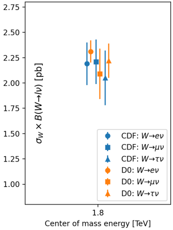

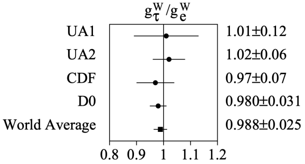

LEP-II

- The most precise and the only simultaneous $\mathcal{B}(W \to e\nu, \mu\nu, \tau\nu)$ measurement prior to this analysis.
  - OPAL [21],
  - DELPHI [22],
  - L3 [23],
  - ALEPH [24].
- The combined LEP result [25] shows agreement between electron and muon decay channels, but tau channel shows moderate deviation (2.6σ) from the average,

$$\frac{2B(W \to \tau\nu_\tau)}{B(W \to e\nu_e) + B(W \to \mu\nu_\mu)} = 1.066 \pm 0.025$$

- compare with the SM prediction 0.999 [26, 27, 28].

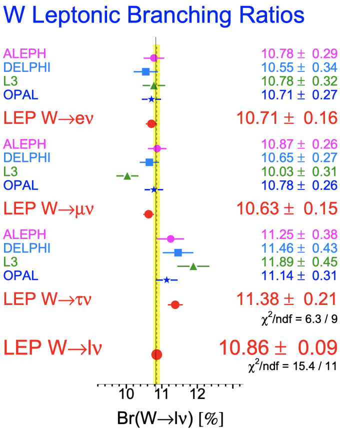

LHC

Run 1

At $\sqrt{s} = 7$ TeV and 8 TeV, the LFU between $W \to e\nu$ and $W \to \mu\nu$ was tested by ATLAS [29] and LHCb [30, 31]:

- Measure W+jets cross-section in electron and muon channels
- Measure ratio of branching fractions:
  - ATLAS: $R_{\mu/e} = 1.003 \pm 0.010$
  - LHCb: $R_{\mu/e} = 0.980 \pm 0.018$.

Run 2

At $\sqrt{s} = 13$ TeV, ATLAS [32] recently published the most precise measurement of $R_{\tau/\mu}$.

- Uses full Run 2 dataset (137 fb^{-1})
- Use $t\bar{t}$ events selected with $\mu\mu$ and $e\mu$ final states with two b-tagged jets
- τ leptons are probed via their muonic final state $\tau \to \mu\bar{\nu}_\mu\nu_\tau$, softer and more displaced than prompt ones.
- Fit the muon transverse impact parameter in three p_T bins
- Measure ratio $R_{\tau/\mu} = 0.992 \pm 0.013$ consistent with LFU.

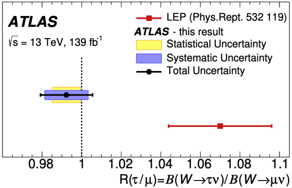

Measuring the W branching fractions with CMS

- **Motivations:**
  - The $\mathcal{B}(W \to e, \mu, \tau)$ measurements have not been improved since the LEP combination,
  - LEP's $R_{\tau/(e,\mu)}$ shows a 2.6 σ deviation from the SM prediction.
- **Opportunities:**
  - LHC 13 TeV collisions produce a large number of $t\bar{t}$ events giving WW pairs
  - The b tagging allows to selection of high purity $t\bar{t}$ sample
  - Improved τ_h identification enables to efficient selection of $W \to \tau\nu$ decays

Interesting processes @LHC

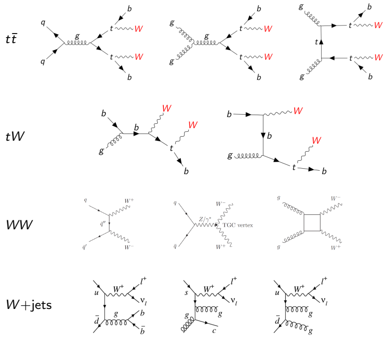

Analysis strategy overview

- Simultaneously measure the three leptonic and inclusive hadronic W branching fractions using data collected CMS
- Target $t\bar{t}$ as primary signal process, also account for tW, WW, and W+jet
- Discriminate between $W \to e/\mu$ and $W \to \tau \to e/\mu$

W decay modes

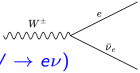

$\mathcal{B}(W \to e\nu)$

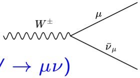

$\mathcal{B}(W \to \mu\nu)$

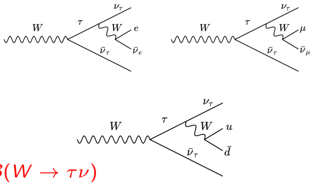

$\mathcal{B}(W \to \tau\nu)$

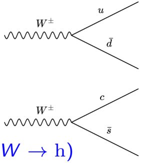

$\mathcal{B}(W \to \mathrm{h})$

Additional derived quantities

- assume partial LFU between e and μ $\Rightarrow$ measure the ratio $R^{W}_{\tau/(e,\mu)}$;
- assume LFU $\Rightarrow$ measure the average leptonic branching fraction, $\mathcal{B}(W \to \ell\nu)$, and inclusive hadronic branching fraction, $\mathcal{B}(W \to \mathrm{h})$;
- assume LFU $\Rightarrow$ derive the SM quantities α_S, $\sum_{d,s,b}^{\mathrm{u,c}} |\mathrm{V}_{ij}|^2$, and $|\mathrm{V}_{cs}|$ from $\mathcal{B}(W \to \mathrm{h})$.

Datasets

Data

- $\mathcal{L} = 35.9\,\mathrm{fb}^{-1}$ dataset collected by CMS during 2016 run
- Two single lepton triggered data streams are used:
  - trigger on muon with $p_T > 24$ GeV
  - trigger on electron with $p_T > 27$ GeV

Simulated data

- signal processes:
  - $t\bar{t}$, tW, WW, W+jets
- background processes:
  - Z+jets, WZ, ZZ, γ+jets
- detils of corrections and calibrations in backup

Data-driven multijet QCD background estimate

- QCD backgrounds are estimated using data-driven methods:
  - Same-sign dilepton sideband used for $e\tau$, $\mu\tau$, and $e\mu$ channels
  - Anti-isolated sideband used for eh and μh
- contamination from prompt leptons estimated from simulation

Event categorization

Baseline selection

- One muon with $p_T > 25$ GeV **OR** one electron with $p_T > 30$ GeV
- Select events with additional electrons, muons, hadronic tau leptons, or jets
- Overlap in object reconstruction prioritizes $\mu \to e \to \tau_h \to h$
- Details of individual object selection in backup

trigger	label	N_e	N_μ	N_{τ_h}	N_j	$N_{b\ tags}$	additional requirements
e	ee	2	0	0	≥ 2	≥ 1	$p_{T,e} > 30$ GeV, $p_{T,e} > 20$ GeV, $\lvert M_{ee} - M_Z \rvert > 15$ GeV
	$e\mu$	1	1	0	≥ 0	≥ 0	$p_{T,e} > 30$, 10 GeV
	$e\tau_h$	1	0	1	≥ 0	≥ 0	$p_{T,e} > 30$ GeV, $p_{T,\tau_h} > 20$ GeV
	eh	1	0	0	≥ 4	≥ 1	$p_{T,e} > 30$ GeV, $p_{T,j} > 30$ GeV
μ	μe	1	1	0	≥ 0	≥ 0	$p_{T,\mu} > 25$, $p_{T,e} > 20$ GeV
	$\mu\mu$	0	2	0	≥ 2	≥ 1	$p_{T,\mu} > 25, 10$ GeV, $\lvert M_{\mu\mu} - M_Z \rvert > 15$ GeV
	$\mu\tau_h$	0	1	1	≥ 0	≥ 0	$p_{T,\mu} > 25$ GeV, $p_{T,\tau_h} > 20$ GeV
	μh	0	1	0	≥ 4	≥ 1	$p_{T,\mu} > 25$ GeV, $p_{T,j} > 30$ GeV

Event categorization

Categorization by N_{jets} and $N_{b\,tags}$

- main selection isolates $t\bar{t}$ and tW production
- finer binning of $\ell\tau$ categories improves purity of hadronic τ ID
- enriched in $Z \to \tau\tau$ used for reducing τ reconstruction systematic uncertainties
- WW events
- additional $t\bar{t}/tW$ events

	$N_j = 0$	$N_j = 1$	$N_j = 2$	$N_j = 3$	$N_j \geq 4$
$N_b = 0$	$e\tau_h$, $\mu\tau_h$, $e\mu$	$e\tau_h$, $\mu\tau_h$, $e\mu$	$e\tau_h$, $\mu\tau_h$, $e\mu$		
$N_b = 1$		$e\tau_h$, $\mu\tau_h$, $e\mu$	$e\tau_h$, $\mu\tau_h$	$e\tau_h$, $\mu\tau_h$	
			ee, $\mu\mu$, $e\mu$		
					eh, μh
$N_b \geq 2$			$e\tau_h$, $\mu\tau_h$	$e\tau_h$, $\mu\tau_h$	
			ee, $\mu\mu$, $e\mu$		
					eh, μh

Discriminating $W \to e/\mu$ vs. $W \to \tau \to e/\mu$

- Features are selected to best isolate $W \to \tau$ decays
  - $W \to \tau \to e/\mu$ tend to have lower transverse momentum
- More sophisticated discrimination techniques considered, e.g. neural networks, but...
  - lepton p_T is by far still strongest source of discrimination "out-of-the-box"
  - additional observables complicates handling systematic uncertainties
- Histograms binning are generated using the Bayesian Block algorithm (arXiv:1708.00810)

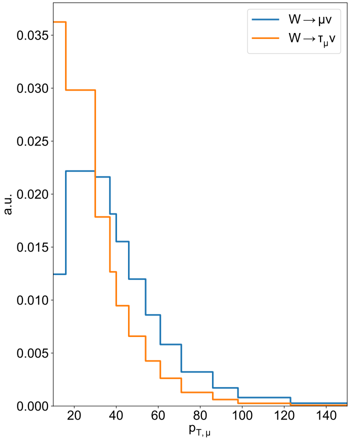

Parameterization of decay modes

- The parameters of interest are the four branching fraction components, $\{B_e, B_\mu, B_\tau, B_h\}$, subject to the constraint $\sum B_i = 1$.
- Accounting for the τ decay modes, $\{b_e, b_\mu, b_h\}$, this can be written

$$\boldsymbol{\beta} = \{B_e, B_\mu, B_\tau b_e, B_\tau b_\mu, B_\tau b_h, B_h\}.$$

- We are mainly interested in WW-like decays, so the matrix $\mathrm{B} = \boldsymbol{\beta} \otimes \boldsymbol{\beta}$ accounts for each possible decay mode
- Correspondingly, the efficiencies for each decay mode can be written in a matrix, E_{ij} so the total number of signal events given process, s, is,

$$N_s = \sigma_s \mathcal{L} \mathrm{E}_{ij} \mathrm{B}_{ij}.$$

decay mode	reconstruction mode: $\mu\mu$	ee	$e\mu/\mu e$	$\mu\tau$	$e\tau$	μh	eh
ee	–	85.8	–	–	0.6	–	3.6
$\mu\mu$	83.3	–	–	0.3	–	1.6	–
$e\mu$	–	–	86.3	0.5	0.2	3.6	1.6
$\tau_e\tau_e$	–	0.5	–	–	–	–	–
$\tau_\mu\tau_\mu$	0.7	–	–	–	–	–	–
$\tau_e\tau_\mu$	–	–	0.5	–	–	–	–
$\tau_e\tau_h$	–	–	–	–	3.0	–	0.2
$\tau_\mu\tau_h$	–	–	–	3.3	–	0.2	–
$\tau_h\tau_h$	–	–	–	–	–	–	–
$e\tau_e$	–	13.3	–	–	0.1	–	0.9
$e\tau_\mu$	–	–	5.5	–	0.1	0.2	0.4
$e\tau_h$	–	0.1	–	–	59.0	–	3.5
$\mu\tau_e$	–	–	7.4	0.1	–	0.7	0.1
$\mu\tau_\mu$	15.6	–	–	–	–	0.5	–
$\mu\tau_h$	–	–	0.1	59.2	–	3.5	–
eh	–	0.2	0.1	–	35.1	–	84.9
μh	0.4	–	0.2	34.7	–	84.1	–
$\tau_e h$	–	–	–	–	1.8	–	4.7
$\tau_\mu h$	–	–	–	1.8	–	5.4	–
$\tau_h h$	–	–	–	–	–	–	–
hh	–	–	–	–	–	–	0.1

Estimated from $t\bar{t}$ simulation with $N_j \geq 2$ and $N_b \geq 2$.

Numbers are in percent of total events.

Likelihood construction

The full data model is a mixture of all signal and background processes accounting for systematic uncertainties using nuisance parameters, θ,

$$f_{ij}(\boldsymbol{B}, \boldsymbol{\theta}) = \sum_{s \in sig} s_{ij,s}(\boldsymbol{B}, \boldsymbol{\theta}) + \sum_{b \in bg} b_{ij,b}(\boldsymbol{\theta}).$$

Based on this, a binned, Poisson likelihood is constructed combining all categories and category-specific observables,

$$\mathrm{NLL}(\boldsymbol{B}, \boldsymbol{\theta}|\mathrm{y}) = \sum_{\mathrm{i} \in \mathrm{category}} \sum_{\mathrm{j} \in \mathrm{p_T\,bins}} \left(-y_{ij} \ln(f_{ij}(\boldsymbol{B}, \boldsymbol{\theta})) + f_{ij}(\boldsymbol{B}, \boldsymbol{\theta})\right) + \sum_{k \in n.p.} \pi_\theta(\theta)$$

where the constraint term, $\pi_\theta(\theta)$, accounts for the prefit systematic uncertainties.

Incorporating systematics

- Most uncertainties are accounted for using morphing templates
- MC statistical uncertainty accounted for on a bin-by-bin basis using Barlow-Beeston lite approach
- Correlations between channels is 100% for shared n.p.
- Each n.p. is treated as independent and uncorrelated with other n.p.

Multijet QCD estimation

$e\tau_h$ and $\mu\tau_h$ categories

- Estimated from sideband with same sign $e\tau_h$ or $\mu\tau_h$ pairs
- $SS \to OS$ transfer factor measured separately in $\ell\tau_h$ events with anti-isolated e/μ and $n_j = 0, n_b = 0$.
- Prompt leptons mainly from $Z \to \tau\tau$ and W+jets accounted for in simulation accounted for based on simulation
- $\mu\tau_h$ with $N_j = 0$ used for validation (shown here)

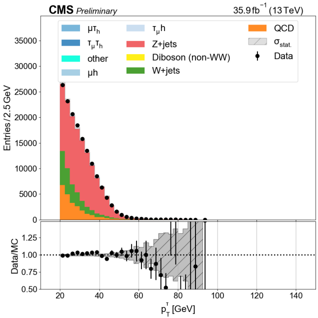

eh and μh categories

- Estimated from sideband anti-isolated leptons.
- Anti-isolated leptons are required to pass loose isolation but fail tight isolation working point.
- Transfer factors $SF^{\overline{\text{iso}}\to\text{iso}}(p_T, \eta)$, measured separately in orthogonal, W+jets control region (ℓh with $1 \leq n_j \leq 3, n_b = 1$).

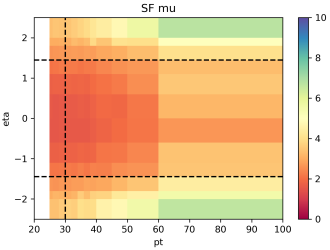

ee and $\mu\mu$: subleading lepton p_T

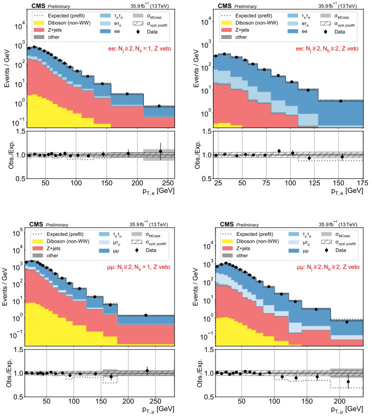

eh and μh lepton p_T

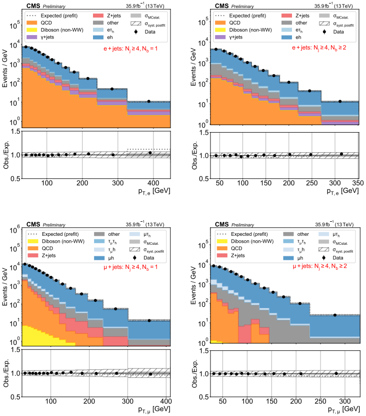

$e\mu$: subleading lepton p_T

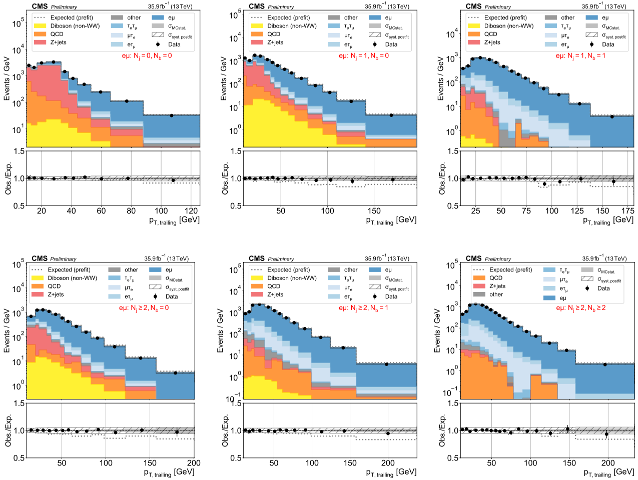

$e\tau_h$: τ_h p_T

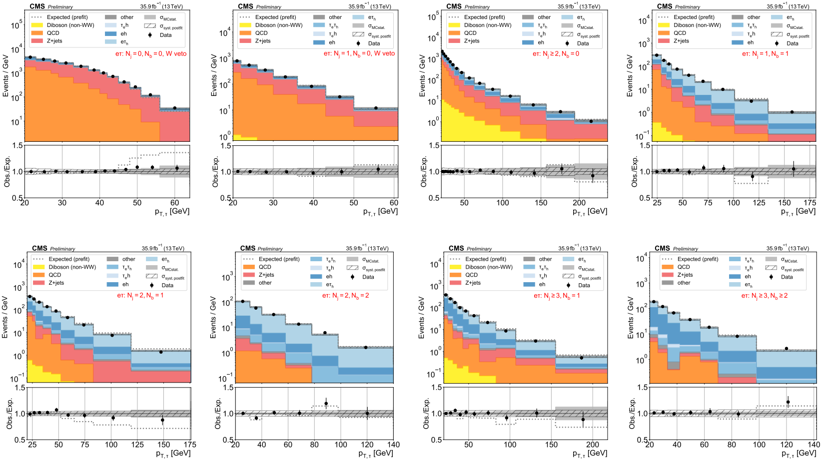

$\mu\tau_h$: τ_h p_T

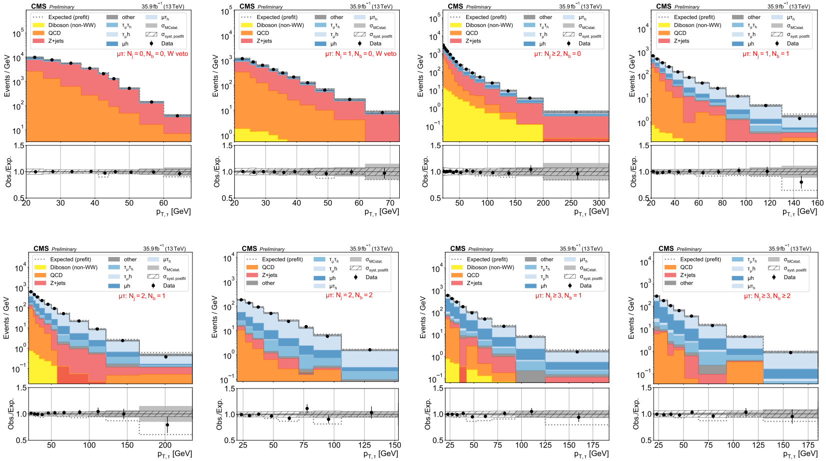

Sources of systematic uncertainties

- Luminosity (2.5%)
- Normalization of simulated processes:
  - tW (10%), γ+jets (10%), VV (10%),
  - $t\bar{t}$, Z+jets, W+jets uncertainty taken from α_S, PDF, and μ_R/μ_F variations
- Data-driven QCD normalization:
  - Same sign estimate ($\ell\tau_h$): 5-30% depending on jet/b tag multiplicity,
  - Anti-isolated leptons (ℓh): 30%
- Generator-level reweightings: PU, top p_T, WW p_T
- Trigger efficiencies: single muon trigger, single electron trigger.
- Object reconstruction:
  - muon: identification, isolation, energy scale.
  - electron: identification, reconstruction, energy scale.
  - tau: identification, misidentification, energy scale.
  - jet: energy scale, energy resolution.
  - btag: tag/mistag.
- Tau decay branching fractions: $\tau \rightarrow e, \mu, h$
- Simulation of $t\bar{t}$: ISR/FSR, matrix element to parton shower matching (ME-PS), underlying event tuning (UE).

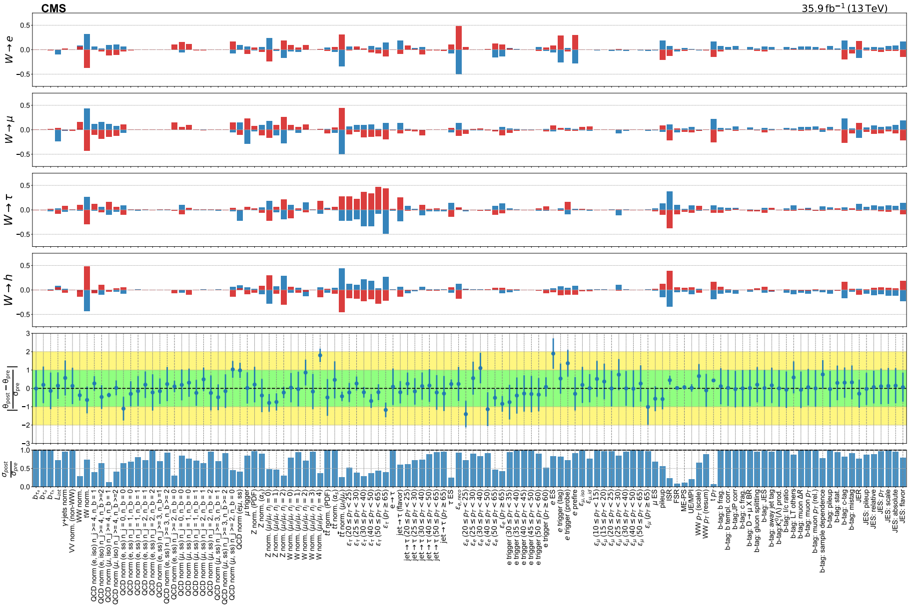

Impacts to the branching fractions are shown in the top four panels as $\Delta B / \sigma_B$.

Bottom two panels show the pulls and constraints $(\sigma_{postfit} / \sigma_{prefit})$, repsectively.

Results: summary plots

- The fit is carried out for three scenarios:
  - each B_ℓ fit independently
  - LFU: $B_e = B_\mu = B_\tau$
  - partial LFU: $B_e = B_\mu \neq B_\tau$
- Contours are drawn assuming a multivariate Gaussian with covariance calculated from the NLL
- Measured values consistent with LFU hypothesis

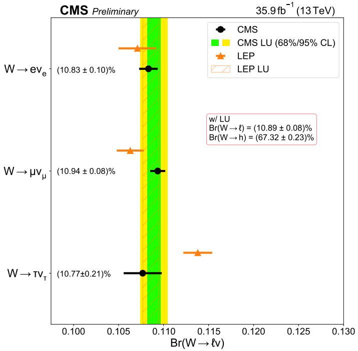

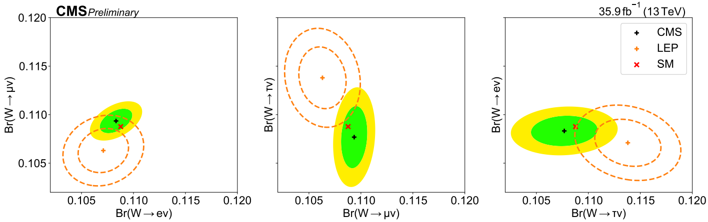

Results: W branching fractions and correlations

	CMS	LEP	CMS+LEP*
w/o LU	($\pm stat. \pm syst.$)	($\pm stat. \pm syst.$)	
$W \to e\nu$	$(\mathbf{10.83} \pm \mathbf{0.01} \pm \mathbf{0.10})\%$	$(10.71 \pm 0.14 \pm 0.07)\%$	$(10.800 \pm 0.085)\%$
$W \to \mu\nu$	$(\mathbf{10.94} \pm \mathbf{0.01} \pm \mathbf{0.08})\%$	$(10.63 \pm 0.13 \pm 0.07)\%$	$(10.883 \pm 0.071)\%$
$W \to \tau\nu$	$(\mathbf{10.77} \pm \mathbf{0.05} \pm \mathbf{0.21})\%$	$(11.38 \pm 0.17 \pm 0.11)\%$	$(11.035 \pm 0.146)\%$
w/ LU			
$W \to h$	$(\mathbf{67.32} \pm \mathbf{0.02} \pm \mathbf{0.23})\%$	$(67.41 \pm 0.18 \pm 0.20)\%$	$(67.365 \pm 0.163)\%$

Correlation matrices for leptonic branching fractions

CMS

$$\begin{bmatrix} 1 & +0.439 & +0.138 \\ +0.439 & 1 & +0.190 \\ +0.138 & +0.190 & 1 \end{bmatrix}$$

LEP

$$\begin{bmatrix} 1 & +0.136 & -0.201 \\ +0.136 & 1 & -0.122 \\ -0.201 & -0.122 & 1 \end{bmatrix}$$

CMS+LEP

$$\begin{bmatrix} 1 & +0.383 & -0.045 \\ +0.383 & 1 & 0.005 \\ -0.045 & 0.005 & 1 \end{bmatrix}$$

*CMS and LEP results are combined assuming no correlations with experimental uncertainties

Results: Ratios of Branching Fractions

- Ratios of branching fractions give a quick check of LFU
- Calculated for each pairing of leptonic branching fractions w/o the LFU assumption,
- The ratio between the τ and e/μ ratios is calculated assuming partial LFU, i.e., $B_e = B_\mu \neq B_\tau$
- details of ratio PDFs in backup

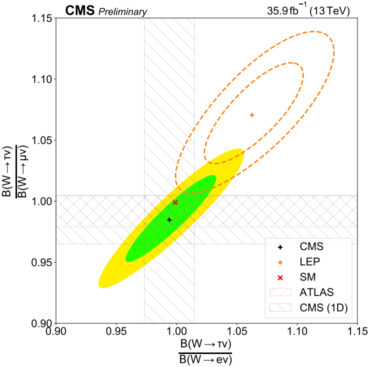

	CMS	LEP	CMS+LEP	ATLAS
$W \to \mu\nu / W \to e\nu$	1.009 ± 0.009	0.993 ± 0.019	1.008 ± 0.008	1.003 ± 0.010
$W \to \tau\nu / W \to e\nu$	0.994 ± 0.021	1.063 ± 0.027	1.022 ± 0.016	–
$W \to \tau\nu / W \to \mu\nu$	0.985 ± 0.020	1.070 ± 0.026	1.014 ± 0.015	0.992 ± 0.013
$2W \to \tau\nu / (W \to e\nu + W \to \mu\nu)$	1.002 ± 0.019	1.066 ± 0.025	1.016 ± 0.015	–

Results: Other SM parameters

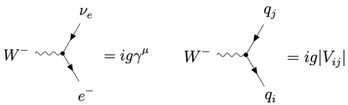

- The measured values of the leptonic branching fractions can also be used as to derive several other quantities of interest including $\alpha_s(M_W)$, $\sum|\mathrm{V}_{ij}|^2$, and V_{cs}.
- These quantities and the hadronic branching fraction are related at NLO by,

$$R_W = \frac{\mathcal{B}(W \to \mathrm{h})}{1 - \mathcal{B}(W \to \mathrm{h})} = \left(1 + \frac{\alpha_S(M_W)}{\pi}\right) \sum_{\substack{i=(\mathrm{u,c}),\\ j=(\mathrm{d,s,b})}} \left|\mathrm{V}_{ij}\right|^2$$

	condition	CMS	LEP	CMS+LEP
R_W	assume LFU	2.060 ± 0.021	2.068 ± 0.025	2.063 ± 0.016
$\alpha_S(M_W)$	assume CKM unitarity	0.094 ± 0.033	0.108 ± 0.040	0.099 ± 0.026
$\sum_{ij}\|V_{ij}\|^2$	use $\alpha_S = 0.112 \pm 0.001$	1.984 ± 0.021	1.992 ± 0.025	1.987 ± 0.016
V_{cs}	CKM matrix element precision measurements	0.967 ± 0.011	0.971 ± 0.013	0.969 ± 0.008

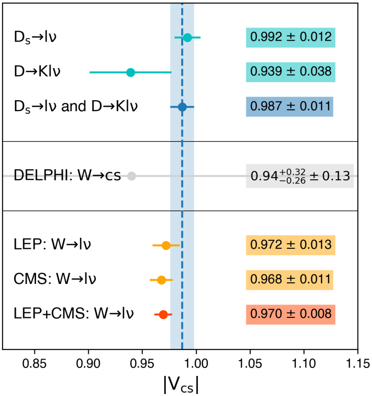

- Our indirect measurement can be compared to direct measurements of $|V_{cs}|$,
  - D_s decays: (Belle [33], CLEO [34, 35, 36], BaBar [37] and BESIII [38, 39])
  - D decays: (Belle [40], CLEO [41], BaBar [42] and BESIII [43, 44])
- The CMS value is as precise as direct measurements and exceeds that precision when combined with the LEP values.

Conclusions

- The leptonic and inclusive hadronic W branching fractions have been determined using data collected by CMS:
  - The precision exceeds the previous best result obtained by LEP,
  - Result is consistent with LU and confirms the recent ATLAS result on the ratio of τ and μ branching fractions,
  - Several additional SM parameters have been derived based on the hadronic branching fraction.
- PAS is available for SMP-18-011
- The paper has finished CWR and will be submitted to PRD

$\mathcal{B}(W \to e\nu)$	$(10.83 \pm 0.10)\%$
$\mathcal{B}(W \to \mu\nu)$	$(10.94 \pm 0.08)\%$
$\mathcal{B}(W \to \tau\nu)$	$(10.77 \pm 0.21)\%$
$\mathcal{B}(W \to \ell\nu)$	$(10.89 \pm 0.08)\%$
$\mathcal{B}(W \to \mathrm{h})$	$(67.32 \pm 0.23)\%$
μ/e	1.009 ± 0.009
τ/e	0.994 ± 0.021
τ/μ	0.985 ± 0.020
$2\tau/(e+\mu)$	1.002 ± 0.019
R_W	2.060 ± 0.021
$\alpha_S(M_W)$	0.094 ± 0.033
$\sum_{d,s,b}^{\mathrm{u,c}} \lvert \mathrm{V}_{ij} \rvert^2$	1.984 ± 0.021
$\lvert \mathrm{V}_{cs} \rvert$	0.967 ± 0.011

BACKUP

Physics object selections

μ

- tight prompt ID and isolation
- $p_T > 25(10)$ GeV
- $|\eta| < 2.4$
- corrections for p_T, ID, iso.

e

- tight prompt ID and isolation
- $p_T > 30(20)$ GeV
- $|\eta| < 2.5$
- corrections for p_T, ID, iso.

τ_h

- MVA isolation w/ decay mode finding
- $p_T > 20$ GeV
- $|\eta| < 2.3$
- corrections for p_T, iso.

jets

- ak4 PFJets with charged hadron subtraction
- loose ID
- veto overlap with e, μ, τ_h
- $p_T > 30$ GeV
- $|\eta| < 2.4$
- corrections for energy scale and resolution applied

b tagging

- medium WP for combined secondary vertex algorithm
- corrections applied for tag/mistag efficiency

Event yields

	QCD	Diboson (non-WW)	WW	Z	W	tW	$t\bar{t}$	Expected	Observed
ee									
$N_j \geq 2, N_b = 0$	–	1014.2 ± 104.7	804.9 ± 46.8	55026.7 ± 5713.1	175.2 ± 25.0	854.4 ± 58.0	10865.1 ± 609.1	68740.4 ± 5747.0	68657
$N_j \geq 2, N_b = 1$	–	119.6 ± 12.4	51.2 ± 4.3	5207.9 ± 579.0	10.1 ± 4.8	1415.3 ± 89.8	24815.2 ± 1388.9	31619.1 ± 1507.5	30332
$N_j \geq 2, N_b \geq 2$	–	17.2 ± 1.8	3.3 ± 0.8	504.9 ± 86.2	5.2 ± 3.7	384.5 ± 30.8	14121.1 ± 791.1	15036.2 ± 796.4	14646
$\mu\mu$									
$N_j \geq 2, N_b = 0$	–	2628.2 ± 271.0	1944.1 ± 110.6	194725.6 ± 20123.0	455.9 ± 43.1	2081.2 ± 127.6	28399.5 ± 1589.3	230234.5 ± 20188.2	238485
$N_j \geq 2, N_b = 1$	–	324.9 ± 33.6	128.4 ± 8.9	19150.5 ± 2023.9	80.0 ± 16.4	3469.2 ± 205.5	64582.6 ± 3612.0	87735.6 ± 4145.7	86354
$N_j \geq 2, N_b \geq 2$	–	48.3 ± 5.0	5.8 ± 1.1	2028.9 ± 253.5	5.3 ± 3.8	976.6 ± 65.4	36916.5 ± 2065.4	39981.3 ± 2082.0	40011
$e\mu$									
$N_j = 0, N_b = 0$	4264.9 ± 285.7	748.9 ± 77.6	17566.8 ± 983.8	49838.9 ± 5152.2	3713.1 ± 262.4	3305.7 ± 196.0	9606.0 ± 538.7	89044.3 ± 5291.3	90784
$N_j = 1, N_b = 0$	1907.5 ± 164.2	774.1 ± 80.2	7384.9 ± 414.6	13584.5 ± 1424.6	1700.9 ± 131.7	5413.8 ± 313.9	25755.0 ± 1441.5	56520.8 ± 2104.4	55427
$N_j = 1, N_b = 1$	279.7 ± 42.4	21.2 ± 2.5	173.9 ± 11.4	712.9 ± 98.8	95.5 ± 18.5	6330.4 ± 365.2	32341.1 ± 1809.6	39954.7 ± 1849.4	39021
$N_j \geq 2, N_b = 0$	737.0 ± 95.6	582.4 ± 60.4	2780.4 ± 157.3	5280.2 ± 574.9	710.3 ± 60.7	3117.8 ± 185.5	40246.2 ± 2251.5	53454.4 ± 2340.0	50301
$N_j \geq 2, N_b = 1$	403.7 ± 60.4	47.0 ± 5.2	185.6 ± 12.1	605.3 ± 89.0	64.9 ± 13.2	5127.5 ± 298.0	91534.6 ± 5118.7	97968.5 ± 5128.5	93440
$N_j \geq 2, N_b \geq 2$	203.0 ± 29.2	4.2 ± 0.6	13.1 ± 1.8	61.8 ± 23.9	14.7 ± 6.1	1510.7 ± 95.4	52401.6 ± 2931.1	54209.1 ± 2932.9	53859
e + jets									
$N_j \geq 2, N_b = 1$	13189.3 ± 740.4	578.8 ± 59.7	65.2 ± 5.2	13637.7 ± 1442.7	46769.4 ± 2637.7	17675.4 ± 999.7	371951.7 ± 20794.5	463867.6 ± 21047.6	468222
$N_j \geq 2, N_b \geq 2$	4665.8 ± 263.9	104.4 ± 10.8	7.1 ± 1.3	2367.0 ± 279.5	6359.5 ± 378.1	7591.6 ± 435.9	256643.9 ± 14348.6	277739.3 ± 14365.3	276116
μ + jets									
$N_j \geq 2, N_b = 1$	42676.6 ± 2389.3	458.4 ± 47.3	90.1 ± 6.7	10504.3 ± 1123.2	71625.7 ± 4028.2	26161.6 ± 1474.4	572088.3 ± 31982.5	723605.0 ± 32376.7	710650
$N_j \geq 2, N_b \geq 2$	13244.3 ± 743.9	82.9 ± 8.6	9.0 ± 1.5	1738.4 ± 219.6	9522.0 ± 555.9	11251.4 ± 640.8	397617.9 ± 22229.3	433465.8 ± 22259.0	429861

Event yields

	QCD	Diboson (non-WW)	WW	Z	W	tW	$t\bar{t}$	Expected	Observed
$e\tau$									
$N_j = 0, N_b = 0$	14609.7 ± 843.7	11.7 ± 1.4	102.2 ± 7.2	30670.4 ± 3175.9	9505.8 ± 594.4	11.1 ± 3.7	29.7 ± 2.8	54940.5 ± 3339.4	55591
$N_j = 1, N_b = 0$	1512.7 ± 125.2	10.0 ± 1.2	20.9 ± 2.3	3237.1 ± 355.2	1159.9 ± 98.0	20.8 ± 5.2	76.3 ± 5.7	6037.5 ± 389.2	6074
$N_j \geq 2, N_b = 0$	5519.7 ± 363.2	233.6 ± 24.3	269.8 ± 16.8	6721.8 ± 724.1	6906.0 ± 410.6	551.2 ± 40.4	5933.6 ± 333.3	26135.7 ± 968.7	25788
$N_j = 1, N_b = 1$	789.5 ± 77.4	8.0 ± 1.0	16.4 ± 2.0	725.6 ± 99.6	650.5 ± 60.3	675.5 ± 47.6	3381.9 ± 190.7	6247.5 ± 241.2	6256
$N_j = 2, N_b = 1$	421.6 ± 59.9	11.7 ± 1.3	10.8 ± 1.6	424.7 ± 69.2	305.0 ± 33.4	538.3 ± 39.7	5994.7 ± 336.8	7706.7 ± 352.8	7388
$N_j \geq 3, N_b = 1$	315.4 ± 56.0	13.1 ± 1.5	5.0 ± 1.0	212.1 ± 42.9	169.3 ± 23.1	302.1 ± 25.7	6021.4 ± 338.2	7038.5 ± 347.2	6660
$N_j = 2, N_b \geq 2$	48.4 ± 16.4	1.1 ± 0.2	0.3 ± 0.2	18.8 ± 15.9	10.6 ± 5.8	83.4 ± 11.1	2606.9 ± 147.4	2769.5 ± 149.7	2683
$N_j \geq 3, N_b \geq 2$	81.3 ± 28.8	1.8 ± 0.3	0.3 ± 0.2	55.2 ± 14.0	18.0 ± 6.9	87.8 ± 11.5	3574.9 ± 201.5	3819.4 ± 204.5	3704
$\mu\tau$									
$N_j = 0, N_b = 0$	19581.5 ± 1133.6	27.6 ± 3.1	244.6 ± 15.3	103926.9 ± 10727.5	20342.3 ± 1205.2	19.3 ± 5.0	66.2 ± 5.1	144208.5 ± 10854.4	146128
$N_j = 1, N_b = 0$	2255.6 ± 167.9	24.0 ± 2.6	37.0 ± 3.4	8216.3 ± 868.5	2470.3 ± 177.3	33.8 ± 6.8	162.4 ± 10.6	13199.4 ± 902.2	13293
$N_j \geq 2, N_b = 0$	5467.2 ± 372.9	313.5 ± 32.5	413.2 ± 24.9	10752.1 ± 1139.7	10989.1 ± 640.3	879.2 ± 59.4	9261.1 ± 519.4	38075.4 ± 1457.1	38184
$N_j = 1, N_b = 1$	1452.3 ± 113.6	12.3 ± 1.4	27.8 ± 2.8	1632.3 ± 193.8	1199.1 ± 96.4	1112.9 ± 72.6	5266.7 ± 296.1	10703.3 ± 390.8	10628
$N_j = 2, N_b = 1$	709.7 ± 75.4	17.6 ± 1.9	18.1 ± 2.1	708.4 ± 101.7	568.1 ± 50.5	769.3 ± 53.1	9493.5 ± 532.4	12284.6 ± 552.1	12048
$N_j \geq 3, N_b = 1$	438.5 ± 70.7	19.5 ± 2.1	9.7 ± 1.5	384.5 ± 62.6	292.9 ± 32.0	480.7 ± 36.5	9413.5 ± 527.9	11039.3 ± 538.5	10314
$N_j = 2, N_b \geq 2$	111.1 ± 19.9	1.7 ± 0.2	1.0 ± 0.4	58.6 ± 23.6	56.0 ± 16.9	153.8 ± 16.5	4157.7 ± 234.1	4539.9 ± 237.3	4321
$N_j \geq 3, N_b \geq 2$	117.5 ± 35.6	3.0 ± 0.4	1.4 ± 0.5	79.4 ± 22.2	18.1 ± 6.9	157.9 ± 16.7	5599.2 ± 314.7	5976.5 ± 318.0	5705

Counting analysis

For each of the trigger and n_b regions, construct ratios $\{X_e, X_\mu, X_\tau\}$ from data with background subtracted $n = N_{\mathrm{data}} - \sum N_{\mathrm{bg}}$,

	Single-μ Trigger		Single-e Trigger	
	$n_b = 1$	$n_b \geq 2$	$n_b = 1$	$n_b \geq 2$
channels	μe, $\mu\mu$, $\mu\tau_h$, μh		ee, $e\mu$, $e\tau_h$, eh	
ratios, $t \in \{\mu, e\}$	$\frac{n^{te}}{n^{te}+n^{t\mu}+n^{t\tau}+n^{th}} = X_e = \frac{E_{ij}^{te}B_{ij}}{E_{ij}^{te}B_{ij}+E_{ij}^{t\mu}B_{ij}+E_{ij}^{t\tau}B_{ij}+E_{ij}^{th}B_{ij}}$ $\frac{n^{t\mu}}{n^{te}+n^{t\mu}+n^{t\tau}+n^{th}} = X_\mu = \frac{E_{ij}^{t\mu}B_{ij}}{E_{ij}^{te}B_{ij}+E_{ij}^{t\mu}B_{ij}+E_{ij}^{t\tau}B_{ij}+E_{ij}^{th}B_{ij}}$ $\frac{n^{t\tau}}{n^{te}+n^{t\mu}+n^{t\tau}+n^{th}} = X_\tau = \frac{E_{ij}^{t\tau}B_{ij}}{E_{ij}^{te}B_{ij}+E_{ij}^{t\mu}B_{ij}+E_{ij}^{t\tau}B_{ij}+E_{ij}^{th}B_{ij}}$			

One gets a system of three quadratic equations with three unknowns $\{\beta_e, \beta_\mu, \beta_\tau\}$,

$$F_e(\beta_e, \beta_\mu, \beta_\tau) = c_{e1}\beta_e^2 + c_{e2}\beta_\mu^2 + c_{e3}\beta_\tau^2 + c_{e4}\beta_e\beta_\mu + c_{e5}\beta_e\beta_\tau + c_{e6}\beta_\mu\beta_\tau + c_{e7}\beta_e + c_{e8}\beta_\mu + c_{e9}\beta_\tau + c_{e0} = 0,$$
$$F_\mu(\beta_e, \beta_\mu, \beta_\tau) = c_{\mu1}\beta_e^2 + c_{\mu2}\beta_\mu^2 + c_{\mu3}\beta_\tau^2 + c_{\mu4}\beta_e\beta_\mu + c_{\mu5}\beta_e\beta_\tau + c_{\mu6}\beta_\mu\beta_\tau + c_{\mu7}\beta_e + c_{\mu8}\beta_\mu + c_{\mu9}\beta_\tau + c_{\mu0} = 0,$$
$$F_\tau(\beta_e, \beta_\mu, \beta_\tau) = c_{\tau1}\beta_e^2 + c_{\tau2}\beta_\mu^2 + c_{\tau3}\beta_\tau^2 + c_{\tau4}\beta_e\beta_\mu + c_{\tau5}\beta_e\beta_\tau + c_{\tau6}\beta_\mu\beta_\tau + c_{\tau7}\beta_e + c_{\tau8}\beta_\mu + c_{\tau9}\beta_\tau + c_{\tau0} = 0,$$

where the coefficients $\{c_{ek}, c_{\mu k}, c_{\tau k}\}$ with $k \in \{0, 1, 2, \dots 9\}$ are fully determined by efficiencies E and data ratios $\{X_e, X_\mu, X_\tau\}$.

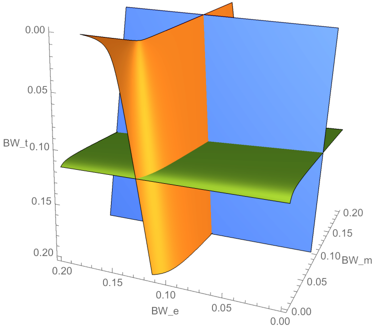

- In the $\{\beta_e, \beta_\mu, \beta_\tau\}$ space, three quadratic equations are three hyperbolic planes, intersection of which is the solution:

$$\begin{bmatrix} \beta_e \\ \beta_\mu \\ \beta_\tau \end{bmatrix} = \text{Sol} \begin{bmatrix} F_e(\beta_e, \beta_\mu, \beta_\tau) = 0 \\ F_\mu(\beta_e, \beta_\mu, \beta_\tau) = 0 \\ F_\tau(\beta_e, \beta_\mu, \beta_\tau) = 0 \end{bmatrix}$$

- The results from different trigger and n_b categories are analytically combined by χ^2 considering the uncorrelated statistical errors and correlated systematic errors.

anti-isolated region

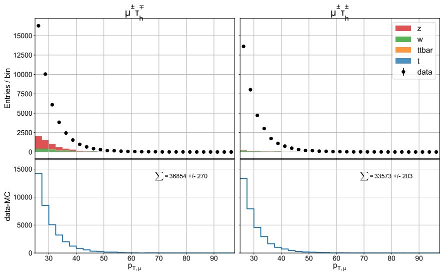

isolated region

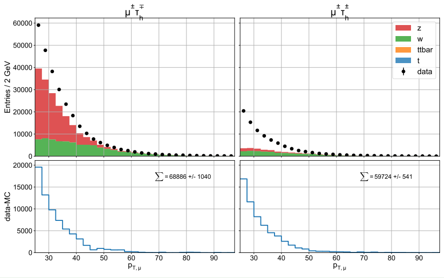

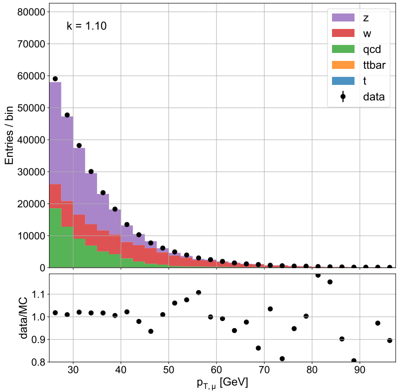

- scale factor (OS/SS) derived from anti-isolated region and applied to isolated region
- can do the same to map anti-isolated OS region to OS isolated region, i.e.,

$$k' = \frac{\text{SS anti-isolated}}{\text{SS isolated}}$$

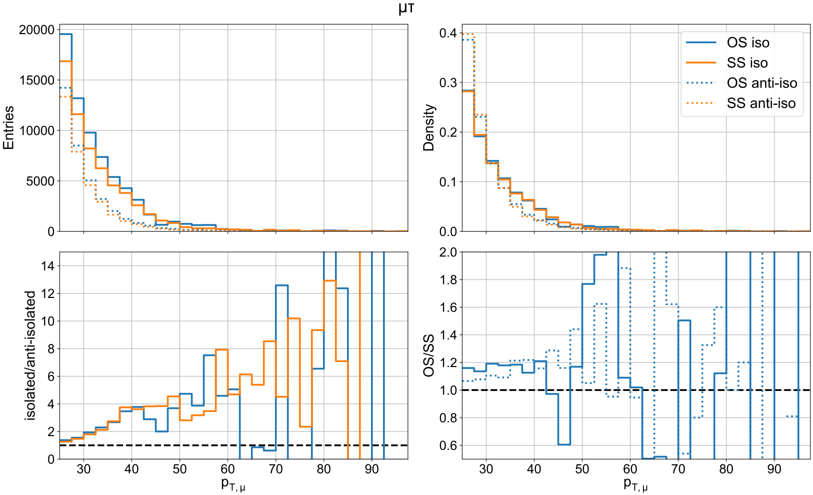

- lower right panel gives scale factors for mapping anti-isolated electrons to signal region

- Bias tests are carried out to confirm the accuracy of the measurement of the branching fractions
- This is done by generating toy data from the Asimov data while accounting for variations of the bin content statistics and nuisance parameters' uncertainty
- Each toy is generated while the leptonic branching fractions are varied on a 10 × 10 × 10 grid of values

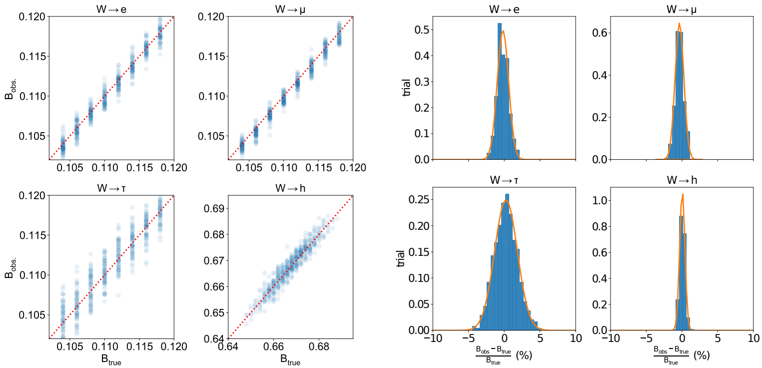

$$\chi^2 = \frac{1}{2}(\beta_{CMS} - \hat{\beta})^T \Sigma_{CMS}^{-1}(\beta_{CMS} - \hat{\beta}) + \frac{1}{2}(\beta_{LEP} - \hat{\beta})^T \Sigma_{LEP}^{-1}(\beta_{LEP} - \hat{\beta}).$$

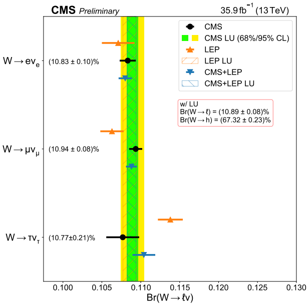

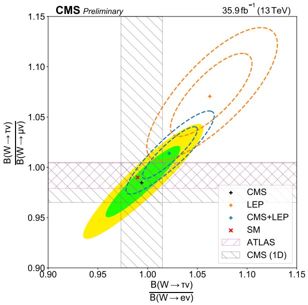

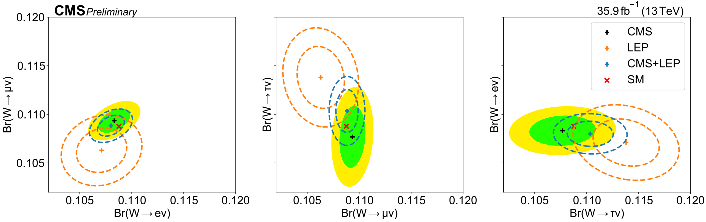

PDF of ratios in 2D

- the 1D and 2D PDFs for the ratios can be calculated analytically by the following transformation[1],
- The values of β_ℓ in the following expression are the MLE estimate. The values of σ and ρ correspond to the standard error and correlation coefficients.

$$f(r) = \int_{-\infty}^{\infty} |B_\ell| \, g(rB_\ell, B_\ell) \, dB_\ell$$

$$f(r_{e\tau}, r_{\mu\tau}) = \frac{bd}{2\pi\sigma_e\sigma_\mu\sigma_\tau a^3}\left[\Phi\left(\frac{b}{a\sqrt{\Psi}}\right) - \Phi\left(\frac{b}{a\sqrt{\Psi}}\right)\right] + \frac{\sqrt{\Psi}}{\sqrt{2\pi^3}\sigma_e\sigma_\mu\sigma_\tau} e^{-\frac{c}{2\Psi}} \tag{1}$$

$$\Psi = 1 - \rho_{e\mu}^2 - \rho_{e\tau}^2 - \rho_{\mu\tau}^2 + 2\rho_{e\mu}\rho_{e\tau}\rho_{\mu\tau}$$

$$\begin{aligned} a \equiv a(r_{e\tau}, r_{\mu\tau}) = & \frac{r_{e\tau}^2(1-\rho_{\mu\tau})}{\sigma_e^2} + \frac{r_{\mu\tau}^2(1-\rho_{e\tau})}{\sigma_\mu^2} + \frac{(1-\rho_{e\mu})}{\sigma_\tau^2} \\ & + \frac{2r_{e\tau}r_{\mu\tau}(\rho_{e\tau}\rho_{\mu\tau} - \rho_{e\mu})}{\sigma_e\sigma_\mu} + \frac{2r_{e\tau}(\rho_{e\mu}\rho_{\mu\tau} - \rho_{e\tau})}{\sigma_e\sigma_\tau} \\ & + \frac{2r_{\mu\tau}(\rho_{e\mu}\rho_{e\tau} - \rho_{\mu\tau})}{\sigma_\mu\sigma_\tau} \end{aligned}$$

[1] Hinkley, D.V. *Biometrika* , Dec., 1969, Vol. 56, No. 3 (Dec., 1969), pp. 635-639

$$b \equiv b(r_{e\tau}, r_{\mu\tau}) = \frac{r_{e\tau}\beta_e (1-\rho_{\mu\tau})}{\sigma_e^2} + \frac{r_{\mu\tau}\beta_\mu (1-\rho_{e\tau})}{\sigma_\mu^2} + \frac{\beta_\tau (1-\rho_{e\mu})}{\sigma_\tau^2}$$
$$+ \frac{(r_{e\tau}\beta_\mu + r_{\mu\tau}\beta_e)(\rho_{e\tau}\rho_{\mu\tau} - \rho_{e\mu})}{\sigma_e\sigma_\mu} + \frac{(r_{e\tau}\beta_\tau + \beta_e)(\rho_{e\mu}\rho_{\mu\tau} - \rho_{e\tau})}{\sigma_e\sigma_\tau}$$
$$+ \frac{(r_{\mu\tau}\beta_\tau + \beta_\mu)(\rho_{e\tau}\rho_{e\mu} - \rho_{\mu\tau})}{\sigma_\mu\sigma_\tau} \tag{2}$$

$$c = \frac{\beta_e^2 (1-\rho_{\mu\tau})}{\sigma_e^2} + \frac{\beta_\mu^2 (1-\rho_{e\tau})}{\sigma_\mu^2} + \frac{\beta_\tau^2 (1-\rho_{e\mu})}{\sigma_\tau^2}$$
$$+ \frac{2\beta_e\beta_\mu (\rho_{e\tau}\rho_{\mu\tau} - \rho_{e\mu})}{\sigma_e\sigma_\mu} + \frac{2\beta_e\beta_\tau (\rho_{e\mu}\rho_{\mu\tau} - \rho_{e\tau})}{\sigma_e\sigma_\tau}$$
$$+ \frac{2\beta_\mu\beta_\tau (\rho_{e\tau}\rho_{e\mu} - \rho_{\mu\tau})}{\sigma_\mu\sigma_\tau} \tag{3}$$

$$d \equiv d(r_{e\tau}, r_{\mu\tau}) = e^{\frac{b^2 - ca^2}{2\Psi a^2}} \tag{4}$$

List of presentations

- first version of fitting analysis: https://indico.cern.ch/event/666748/
- first version of counting analysis: https://indico.cern.ch/event/666749/
- current version: https://indico.cern.ch/event/706254/
- early systematics: https://indico.cern.ch/event/719952/contributions/2959333/
- updated systematics: https://indico.cern.ch/event/727175/
- full systematics: https://indico.cern.ch/event/745825/
- USCMS meeting plenary https://indico.cern.ch/event/700320/contributions/2987445/
- September update https://indico.cern.ch/event/747714/#65-w-branching-ratios
- new categories https://indico.cern.ch/event/753845/#2-w-branching-fractions-update
- statistics committee https://indico.cern.ch/event/770861/#1-smp-18-011

Summary of recent talks

- talk at physics coordination plenary[2]:
  - most issues summed up in post from Guillelmo[3]
- updates to SMP/SMPV in response to issues from PC[456]:
  - presented updates to questions raised during PC plenary
- talk to TOP PAG[7]:
  - requested to add $t\bar{t}$ simulation uncertainties
  - modify top p_T reweighting
- last ARC meeting[8]

---

5 https://indico.cern.ch/event/812673/#3-smp-w-branching-fractions

6 https://twiki.cern.ch/twiki/bin/view/CMS/SMP18011#Comments_from_Guillelmo_et_al_po

7 https://indico.cern.ch/event/815395/#2-update-on-w-br

8 https://indico.cern.ch/event/820492/#10-smp-18-011-w-br-report

9 https://indico.cern.ch/event/835251/#1-update-on-w-decay-branching

10 https://indico.cern.ch/event/820644/#3-w-to-lnu-branching-fractions

11 https://indico.cern.ch/event/811941/#1-smp-18-011-material

Data

Table: Data samples produced by CMS in 2016.

Sample	Run ranges	$L_{int}(fb^{-1})$
SingleMuon/Run2016B-03Feb2017_ver2-v2	272007-275376	5.33
SingleMuon/Run2016C-03Feb2017-v2	275657-276283	2.4
SingleMuon/Run2016D-03Feb2017-v2	276315-276811	4.26
SingleMuon/Run2016E-03Feb2017-v2	276831-277420	4.1
SingleMuon/Run2016F-03Feb2017-v2	277772-278808	3.2
SingleMuon/Run2016G-03Feb2017-v2	278820-280385	7.8
SingleMuon/Run2016H-03Feb2017_ver*-v1	281613-284044	9.2
SingleElectron/Run2016B-03Feb2017_ver2-v2	272007-275376	5.33
SingleElectron/Run2016C-03Feb2017-v2	275657-276283	2.4
SingleElectron/Run2016D-03Feb2017-v2	276315-276811	4.26
SingleElectron/Run2016E-03Feb2017-v2	276831-277420	4.1
SingleElectron/Run2016F-03Feb2017-v2	277772-278808	3.2
SingleElectron/Run2016G-03Feb2017-v2	278820-280385	7.8
SingleElectron/Run2016H-03Feb2017_ver*-v1	281613-284044	9.2

MC samples

- production info: RunIISummer16MiniAODv2-PUMoriond17_80X_mcRun2_asymptotic_2016_TrancheIV_v6-v1
- pileup reweighting applied using $\sigma_{\text{minbias}} = 69.2 \pm 3.2$ mb

- **top**:
  - TT_powheg (inclusive, leptonic, semi-leptonic)
  - ST_tW_antitop_5f_inclusiveDecays_TuneCUETP8M2T4
  - ST_tW_top_5f_inclusiveDecays_TuneCUETP8M2T4
- **Z+jets**:
  - DYJetsToLL_M-10to50_amcatnlo
  - DYJetsToLL_M-50_amcatnlo
- **W+jets**:
  - W1JetsToLNu
  - W2JetsToLNu
  - W3JetsToLNu
  - W4JetsToLNu
- **diboson**
  - WWTo2L2Nu_powheg
  - WZTo2L2Q_amcatnlo
  - WZTo3LNu_powheg
  - ZZTo2L2Nu_powheg
  - ZZTo2L2Q_amcatnlo

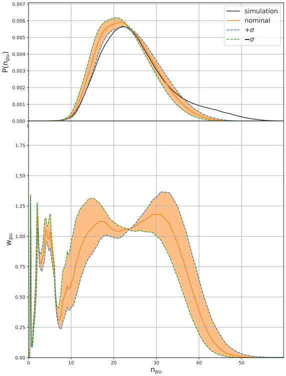

μ selection

- Rochester corrections applied
- $p_T > 25, 10$ GeV
- $|\eta| < 2.4$
- scale factors applied to correct for ID/ISO and trigger efficiencies

variable	cut value
isGlobal	True
isPF	True
χ^2	< 10
number of matched stations	> 1
number of pixel hits	> 0
number of track layers	> 5
number of valid hits	> 0
$\|d_{xy}\|$	< 0.2
$\|d_z\|$	< 0.5
ISO_{PF}/p_T (ρ corrected)	< 0.15

e selection

- $p_T > 10$
- $|\eta| < 2.5$
- scale factors applied for reconstruction/ID efficiencies

variable	$|\eta| < 1.4446$	$|\eta| \geq 1.566$
$\sigma_{i\eta}\sigma_{i\eta}$	< 0.00998	0.0394
$|d\eta|$	< 0.00308	0.0292
$|d\phi|$	< 0.0816	0.00605
H/E	< 0.0414	0.0641
$|\frac{1}{E} - \frac{1}{p}|$	< 0.0129	0.0129
missing hits	≤ 1	*leq*1
$|d_0|$	$< 1.$	$< 1.$
conversion rejection	true	true
ISO_{PF}/p_T (EA corrected)	< 0.0588	< 0.0571

τ selection

- $p_T > 20$ GeV
- $|\eta| < 2.3$
- tight MVA isolation with lifetime
- decay mode finding
- veto taus that overlap with analysis electrons and muons
- assume flat 95% data/MC scale factors; additional corrections will be included in the next iteration

jets

- PFJets, anti-k_t $dR = 0.4$ with CHS
- loose PF ID (see backup)[9]
- $p_T > 30$ GeV
- $|\eta| < 2.4$
- no PUID
- remove overlap with analysis muons, electrons, taus $\Delta R(\ell, j) > 0.4$
- **b tagging**: bMVA > 0.9432[10]
- b jet efficiency accounted for using promotion/demotion method
- jet corrections are propagated to MET (Type-I corrections)

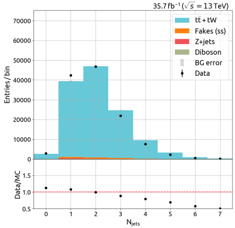

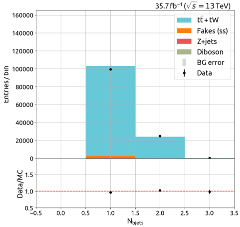

5 https://twiki.cern.ch/twiki/bin/view/CMS/JetID13TeVRun2016

6 https://twiki.cern.ch/twiki/bin/viewauth/CMS/BtagRecommendation80XReReco#Supported_Algorithms_and_Operati

corrections and scale factors

- pileup[11]
- top p_T reweighting ($t\bar{t}$ only)[12]
- muons:[13]
  - trigger efficiency (run dependent)
  - identification/isolation (run dependent)
  - Rochester scale corrections[14]
- electrons:[15]
  - trigger efficiency (taken from authors of EXO-16-049)
  - reconstruction/identification (run dependent)
- taus: flat 0.95 factor[16]
- b jet: tag efficiency[17]

---

11 https://twiki.cern.ch/twiki/bin/view/CMS/PileupJSONFileforData#Pileup_JSON_Files_For_Run_II

12 https://twiki.cern.ch/twiki/bin/view/CMS/TopPtReweighting

13 https://twiki.cern.ch/twiki/bin/view/CMS/MuonWorkInProgressAndPagResults#Results_on_the_full_2016_data

14 https://www-cdf.fnal.gov/ jyhan/cms_momscl/cms_rochcor_manual.html

15 https://twiki.cern.ch/twiki/bin/view/CMS/EgammaIDRecipesRun2#Electron_efficiencies_and_scale

16 https://twiki.cern.ch/twiki/bin/viewauth/CMS/TauIDRecommendation13TeV#Tau_ID_efficiency

17 https://twiki.cern.ch/twiki/bin/viewauth/CMS/BtagRecommendation80XReReco#Supported_Algorithms_and_Operati

Lepton universality tests

- with the branching fractions measured precisely, we can test lepton universality
- this will be done by testing a number of hypotheses:
  - universality (null): $\beta_e = \beta_\mu = \beta_\tau$
  - non-universality (alt. 1): $\beta_e \neq \beta_\mu \neq \beta_\tau$
  - 3rd generation non-universality (alt. 2): $\beta_e = \beta_\mu \neq \beta_\tau$
- this can be assessed by constructing a profile likelihood ratio:

$$\lambda = 2(\ln \mathcal{L}(\theta_{alt}|data) - \ln \mathcal{L}(\theta_{null}|data))$$

- we have done some preliminary tests for null vs. alt. 1 w/ 100 toys
- based on Wilk's Theorem, we would expect this to be distributed as χ^2_2 which seems approximately to be the case
- post-ublinding comment: because the observed values of the branching fractions are so close to the LU assumption, such hypothesis test is unnecessary

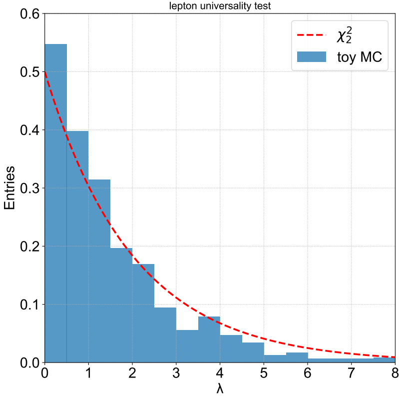

MC statistics: partial Barlow-Beeston

- to account for limited MC statistics, we have adopted the Barlow-Beeston lite approach[18]
- there are 400 bins in total so including a n.p. for each is not quite feasible
- solve for bin-by-bin amplitudes, β, in the objective

$$-\ln \mathcal{L} = -n \ln \beta\mu + \beta\mu + \frac{(\beta - 1)^2}{2\sigma_\beta^2}$$

- effectively does a two-step minimization: once for MC statistics, once for all other systematics
- + can be done analytically +
- - has the issue of "confusing" the minimization -

	e	μ	τ	h
w/o MC stat	0.76	0.55	1.19	0.28
w/ MC stat	0.99	0.72	1.63	0.36

[1] arXiv:1103.0354 §5

percent uncertainties on $B(W \to \ell/h)$

- we considered the effect of individually adding in new categories to fit
- the effect of constraints on shared systematics are not obvious from this study
- when shape information is excluded, the p_T distributions are integrated before evaluating the likelihood

	w/o shape				w/ shape			
	e	μ	τ	h	e	μ	τ	h
baseline	2.04	1.43	5.85	0.93	1.46	1.03	3.28	0.56
$e\tau$ CR	2.00	1.25	4.70	0.80	1.42	0.93	2.69	0.48
$\mu\tau$ CR	1.89	1.22	4.09	0.76	1.37	0.93	2.54	0.47
$\ell\tau$ CR	1.82	1.18	4.05	0.75	1.27	0.88	2.48	0.45
$e\mu$ $t\bar{t}$	1.97	1.28	5.33	0.74	1.31	0.88	3.02	0.45
$e\mu$ WW	2.03	1.43	5.85	0.93	1.39	1.02	3.22	0.53
$e\mu$ $t\bar{t} + WW$	1.96	1.28	5.32	0.73	1.27	0.87	2.99	0.44
combined	1.70	1.02	2.95	0.54	0.99	0.72	1.63	0.36

Lepton $\delta\epsilon$ p_T-dependence

- one of the main requests from the PC plenary was to account for the p_T-dependence of the lepton efficiency uncertainty
- account for this by including additional p_T-dependent n.p.:
  - e: 6 n.p. w/ 1% σ_{pre}
  - μ: 7 n.p. w/ 1% σ_{pre}
  - τ: 6 n.p. w/ 5% σ_{pre}
- p_T binning
  - e & τ: [20, 25, 30, 40, 50, 65, inf.]
  - μ: [10, 20, 25, 30, 40, 50, 65, inf.]
- id+iso/reco uncertainties are still included for e and μ distributions as shape n.p.

	e	μ	τ	h
nominal	0.99	0.72	1.63	0.36
+ e n.p.	1.14	0.73	1.74	0.39
+ μ n.p.	1.03	0.77	1.85	0.39
+ τ n.p.	1.01	0.73	1.75	0.37
+ ℓ n.p.	1.16	0.77	1.91	0.40

Updated HLT_Ele27_WPTight scale factors

- switched to using "official" scale factors
- previously using values calculated for EXO-16-049
- makes accounting for trigger based shape systematics easier (to be done)

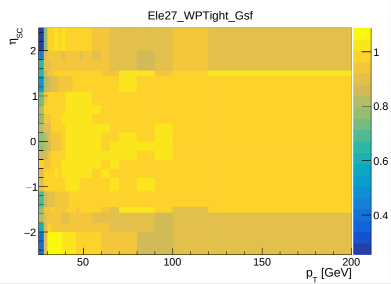

τ branching fractions

- asked to check the hadronic *tau* branching fractions
- still needs to be done, but have verification that the leptonic values diverge from PDG values

decay	simulation	PDG
e	0.17728	0.1782(4)
μ	0.17311	0.1739(4)
$\pi^{\pm}$	0.10768	0.1082(5)
$\pi^{\pm}\pi^{0}$	0.25374	0.2549(9)
$\pi^{\pm}\pi^{0}\pi^{0}$	0.09247	0.0926(10)
$\pi^{\pm}\pi^{\pm}\pi^{\mp}$	0.09257	0.0931(5)
$\pi^{\pm}\pi^{\pm}\pi^{\mp}\pi^{0}$	0.04594	0.0462(5)
5 prong	?	$9.9(4) \times 10^{-4}$

trigger effects

- triggers are accounted for by using normalization n.p.
- this mainly is not a problem since we fit the trailing/non-firing lepton leg
- Ziheng checked contribution

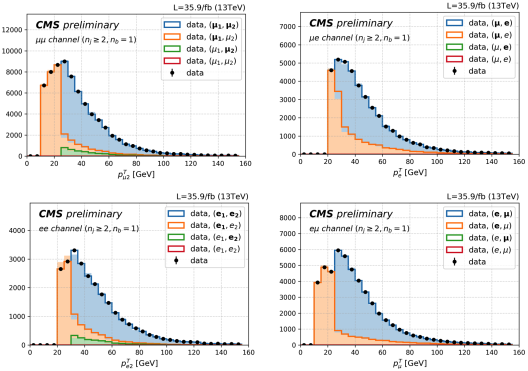

τ to hadrons branching fractions

- based on a comment from Guillelmo, we checked the effect of varying the $\tau \to$ hadrons branching fractions
- the effect is small compared to the total uncertainty, but non-zero

decay mode	PDG	PYTHIA8	weight
$\tau \to \pi^{\pm}$	0.1082(5)	0.1076825	1.00481
$\tau \to \pi^{\pm} + \pi^0$	0.2549(9)	0.2537447	1.00455
$\tau \to \pi^{\pm} + 2\pi^0$	0.0926(10)	0.0924697	1.00141
$\tau \to 3\pi^{\pm}$	0.0931(5)	0.0925691	1.00574
$\tau \to 3\pi^{\pm} + \pi^0$	0.0462(5)	0.0459365	1.00574

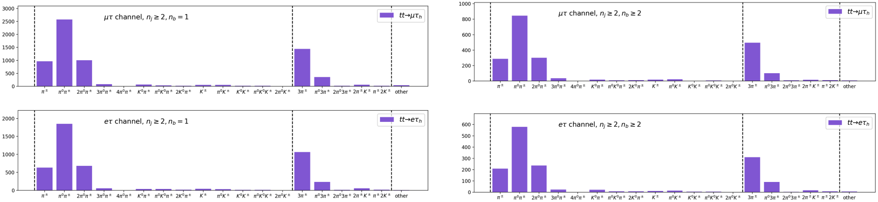

$gg \to WW$

- added $gg \to WW$ process
- accounts for 5% of total contribution
- assume cross section of 0.588 pb
- fully correlated with $qq \to WW \Rightarrow$ not including additional systematic

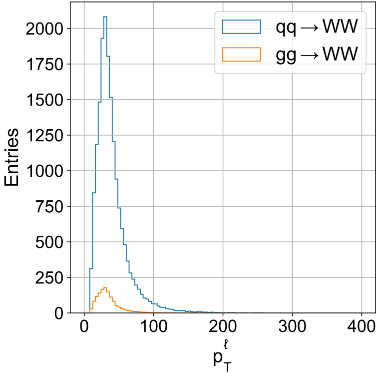

- same reweighting as in WW cross section measurement (SMP-18-004)
- two sources of uncertainty:
  - resummation
  - scale
- effect on $qq \to WW$ template mostly independent of trailing lepton p_T
- only relelvant in WW dominated region, i.e., $e\mu$ with no jets

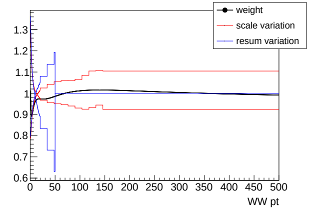

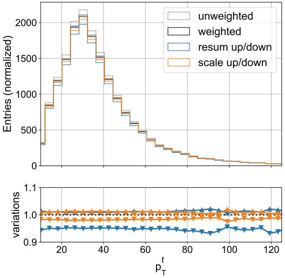

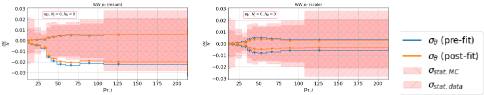

$Z\ p_T$ reweighting

- applied Z p_T reweighting as used in the $H \to WW$ analysis (AN-2017/260)
- not included as an uncertainty (not described in the AN, but authors have been contacted)
- dilepton p_T for the $\mu\mu$ category shown here

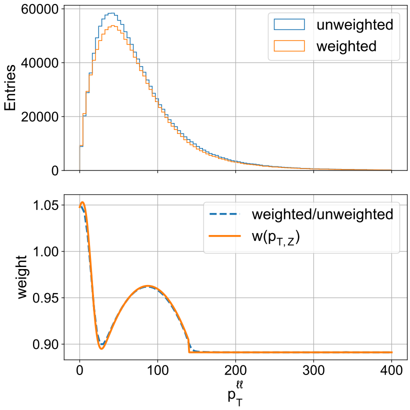

top p_T

- top p_T weights calculated as described on TOP PAG twiki [19]
- as discussed in the last meeting, the weights are not applied, but are used to derive uncertainty envelope
- included in fit as a single nuisance parameter
- nuisance parameter is constrained according to a half Gaussian (positive values only)
- small effect on branching fractions

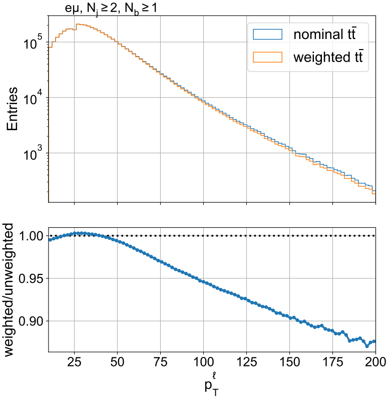

	$W \to e$	$W \to \mu$	$W \to \tau$	$W \to h$
w/o top p_T	0.95	0.75	2.01	0.45
w/ top p_T	0.96	0.75	2.03	0.46

3 https://twiki.cern.ch/twiki/bin/view/CMS/TopPtReweighting

top PS systematics

- several top modeling systematics[20] have been (re)introduced:
  - shower scales (ISR and FSR)
  - ME-PS matching (hdamp parameter)
  - underlying event (variation of CUETP8M2T4 tune)
- systematics for b decays not included (color reconnection, fragmentation, etc.)
- these systematics rely on dedicated samples which are somewhat statistically limited
- included in model as shape nuisance parameters

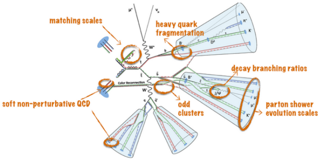

2 https://twiki.cern.ch/twiki/bin/viewauth/CMS/TopSystematics#Factorization_and_renormalizatio

Effect on branching fraction precision

- effect of each systematic is tested relative to the "baseline" precision
- impact is almost exclusively on the precision of $W \to \tau$
- FSR is by the most significant contributor

syst. source	$W \to e$	$W \to \mu$	$W \to \tau$	$W \to h$
baseline	0.98	0.63	1.62	0.33
ISR	0.98	0.63	1.69	0.34
FSR	0.98	0.63	1.97	0.37
ME-PS	0.98	0.63	1.63	0.33
tune	0.98	0.63	1.65	0.33
combined	0.98	0.64	2.01	0.38

Inspecting per bin effect on n.p.

- to further validate the performance of the fitting procedure, we have done some profile likelihood scans
- this is performed by scanning over values of a parameter near its minimum and minimizing the likelihood w.r.t. the remaining parameters
- additionally, the contribution to the curvature (variance) can be estimated for each bin in the fit
- I show the case of the three leptonic branching fractions

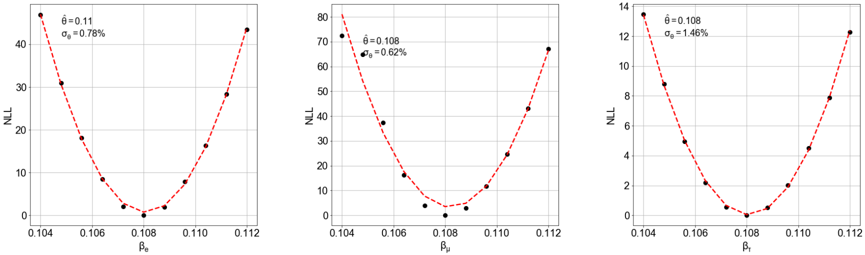

$W \to e$

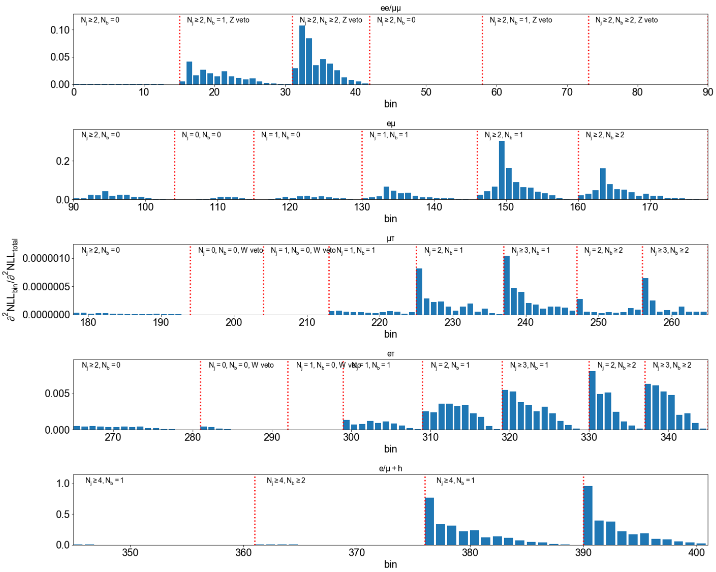

$W \to \mu$

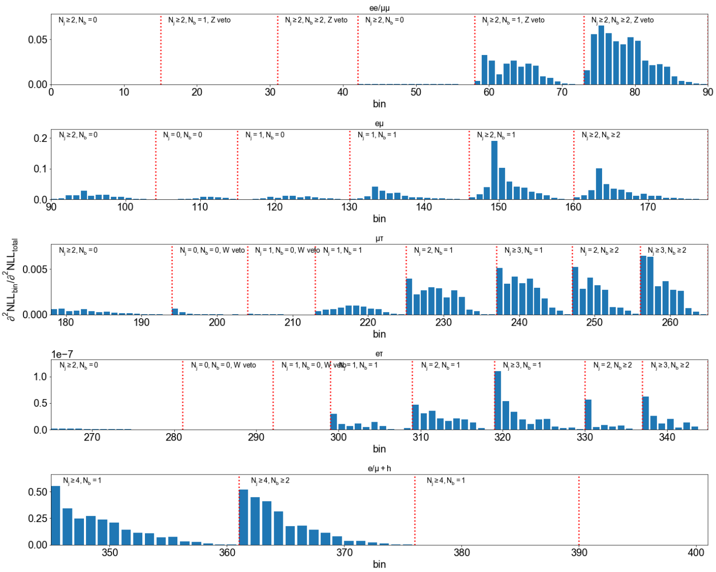

$W \to \tau$

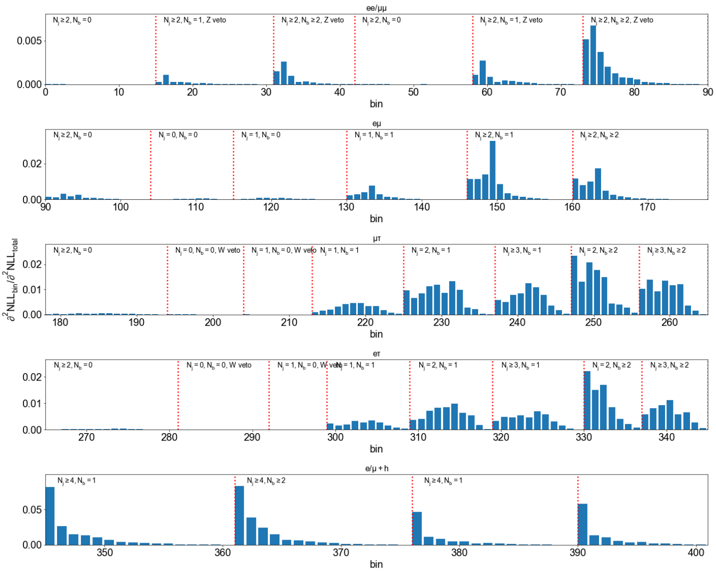
ee/μμ
N_j ≥ 2, N_b = 0
N_j ≥ 2, N_b = 1, Z veto
N_j ≥ 2, N_b ≥ 2, Z veto
N_j ≥ 2, N_b = 0
N_j ≥ 2, N_b = 1, Z veto
N_j ≥ 2, N_b ≥ 2, Z veto
eμ
N_j ≥ 2, N_b = 0
N_j = 0, N_b = 0
N_j = 1, N_b = 0
N_j = 1, N_b = 1
N_j ≥ 2, N_b = 1
N_j ≥ 2, N_b ≥ 2
μτ
N_j ≥ 2, N_b = 0
N_j = 0, N_b = 0, W veto
N_j = 1, N_b = 0, W veto
N_j = 1, N_b = 1
N_j = 2, N_b = 1
N_j ≥ 3, N_b = 1
N_j = 2, N_b ≥ 2
N_j ≥ 3, N_b ≥ 2
eτ
N_j ≥ 2, N_b = 0
N_j = 0, N_b = 0, W veto
N_j = 1, N_b = 0, W veto
N_j = 1, N_b = 1
N_j = 2, N_b = 1
N_j ≥ 3, N_b = 1
N_j = 2, N_b ≥ 2
N_j ≥ 3, N_b ≥ 2
e/μ + h
N_j ≥ 4, N_b = 1
N_j ≥ 4, N_b ≥ 2
N_j ≥ 4, N_b = 1
∂²NLL_bin/∂²NLL_total
bin

pileup n.p.

- pileup ends up being pretty strongly constrained ($\sigma_{post}/\sigma_{pre} \approx 0.5$)
- a likelihood scan has been carried to investigate where this comes from
- it appears that most of the sensitivity is from the e/μ + jet categories
- correlations are attached to indico

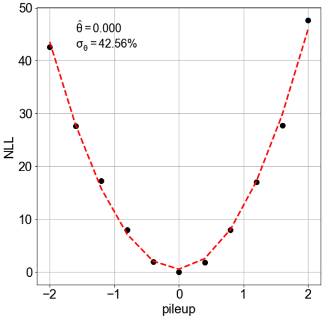

pileup

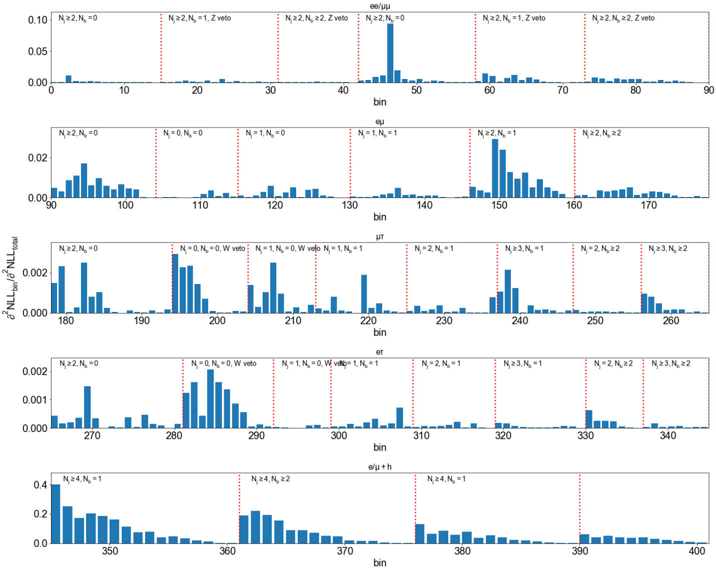
ee/μμ
$N_j \geq 2, N_b = 0$
$N_j \geq 2, N_b = 1$, Z veto
$N_j \geq 2, N_b \geq 2$, Z veto
$N_j \geq 2, N_b = 0$
$N_j \geq 2, N_b = 1$, Z veto
$N_j \geq 2, N_b \geq 2$, Z veto
bin
eμ
$N_j \geq 2, N_b = 0$
$N_j = 0, N_b = 0$
$N_j = 1, N_b = 0$
$N_j = 1, N_b = 1$
$N_j \geq 2, N_b = 1$
$N_j \geq 2, N_b \geq 2$
bin
μτ
$N_j \geq 2, N_b = 0$
$N_j = 0, N_b = 0$, W veto
$N_j = 1, N_b = 0$, W veto
$N_j = 1, N_b = 1$
$N_j = 2, N_b = 1$
$N_j \geq 3, N_b = 1$
$N_j = 2, N_b \geq 2$
$N_j \geq 3, N_b \geq 2$
bin
eτ
$N_j \geq 2, N_b = 0$
$N_j = 0, N_b = 0$, W veto
$N_j = 1, N_b = 0$, W veto
$N_j = 1, N_b = 1$
$N_j = 2, N_b = 1$
$N_j \geq 3, N_b = 1$
$N_j = 2, N_b \geq 2$
$N_j \geq 3, N_b \geq 2$
bin
e/μ + h
$N_j \geq 4, N_b = 1$
$N_j \geq 4, N_b \geq 2$
$N_j \geq 4, N_b = 1$
bin
$\partial^2 NLL_{bin} / \partial^2 NLL_{total}$

$ee/\mu\mu$

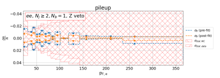
pileup
ee, $N_j \geq 2$, $N_b = 1$, Z veto

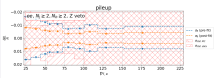
pileup
ee, $N_j \geq 2$, $N_b \geq 2$, Z veto

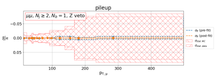
pileup
$\mu\mu$, $N_j \geq 2$, $N_b = 1$, Z veto

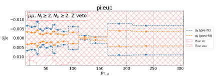
pileup
$\mu\mu$, $N_j \geq 2$, $N_b \geq 2$, Z veto

$e\mu$

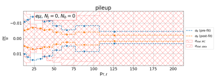
pileup
$e\mu$, $N_j = 0$, $N_b = 0$

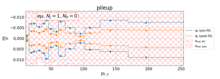
pileup
$e\mu$, $N_j = 1$, $N_b = 0$

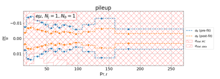
pileup
$e\mu$, $N_j = 1$, $N_b = 1$

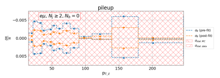
pileup
$e\mu$, $N_j \geq 2$, $N_b = 0$

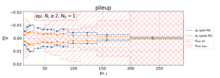
pileup
$e\mu$, $N_j \geq 2$, $N_b = 1$

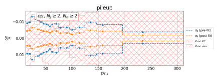
pileup
$e\mu$, $N_j \geq 2$, $N_b \geq 2$

$e\tau$

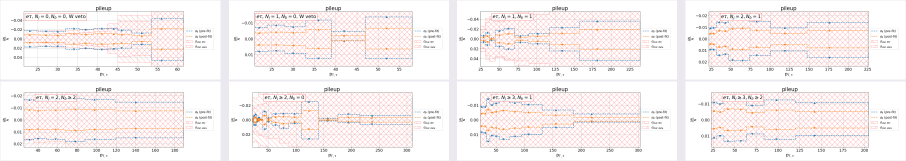
pileup
$e\tau$, $N_j = 0, N_b = 0$, W veto
$e\tau$, $N_j = 1, N_b = 0$, W veto
$e\tau$, $N_j = 1, N_b = 1$
$e\tau$, $N_j = 2, N_b = 1$
$e\tau$, $N_j = 2, N_b \geq 2$
$e\tau$, $N_j \geq 2, N_b = 0$
$e\tau$, $N_j \geq 3, N_b = 1$
$e\tau$, $N_j \geq 3, N_b \geq 2$
$p_{T,\tau}$

$\mu\tau$

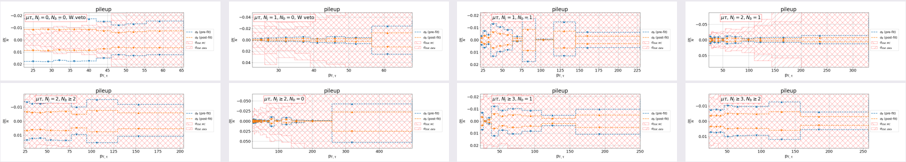
pileup
$\mu\tau$, $N_j = 0, N_b = 0$, W veto
$\mu\tau$, $N_j = 1, N_b = 0$, W veto
$\mu\tau$, $N_j = 1, N_b = 1$
$\mu\tau$, $N_j = 2, N_b = 1$
$\mu\tau$, $N_j = 2, N_b \geq 2$
$\mu\tau$, $N_j \geq 2, N_b = 0$
$\mu\tau$, $N_j \geq 3, N_b = 1$
$\mu\tau$, $N_j \geq 3, N_b \geq 2$
$p_{T,\tau}$

- pileup variation is generally less than the statistical component
- for e/μ + jet categories this variation is larger than the statistical contribution, in particular, for the one b tag category

e jets

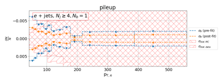

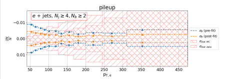

μ jets

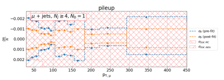

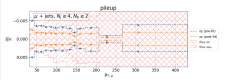

FSR effect on τ ID/misID

- a study has been carried out to isolate the effect of FSR
- since we're mainly interested in the difference between nominal/modified MC samples, the study used MC truth information

method

- match reconstructed τ to generator level τ or jet
- measure efficiency of reconstructed τ to pass MVA ID

Main effect is on the $j \to \tau_h$ misID at the 30% level (*N.B. the nominal misID scale factors are unity and are measured with a* $\sim$ 5% *precision.*)

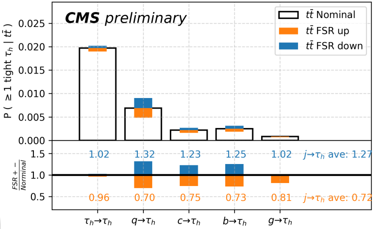

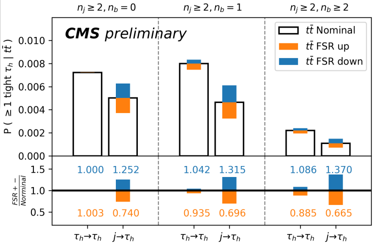

Propagating correction to morphing templates

- the large variation observed in the FSR samples would be corrected out in practice and the scale factors carry a smaller uncertainty (in our studies they were below 5% for both $\tau \rightarrow \tau_h$ and $j \rightarrow \tau_h$ efficiencies)
- following this logic, the MC to MC scale factors in the previous slide are applied to the FSR variation templates when calculating the morphing template
- the average over all categories is used, higher jet/b tag multiplicities do have larger scale factors
- treatment supported by τ POG

	$W \rightarrow e$	$W \rightarrow \mu$	$W \rightarrow \tau$	$W \rightarrow h$
nominal	1.02	0.71	2.04	0.40
w/ τ FSR corrections	1.01	0.69	1.69	0.36

smoothing of template variations for $t\bar{t}$

- as has been noted several times before, the $t\bar{t}$ generator systematics are produced from dedicated samples that have limited statistical precision (even with extensions samples)
- as a result the morphing templates derived from the samples are fairly noisy
- the TOP PAG suggested smoothing the templates
- there is no official statistics committee recomendation for this currently
- possible methods for smoothing:
  - KDE: use instead of histograms, still picks up statistical noise from limited number of events
  - LOWESS: smooths templates based on difference between varied and nominal cases
  - generate toys: used by TOP-17-001, allows for estimation of MC uncertainty as well instead of using Barlow-Beeston lite
- stats committee leans toward LOWESS (based on recent correspondence with TOP-19-008) so I'm using it
- our binning method already confers a degree of smoothing given the bin size correlates with bin occupancy
- examples for some categories in next few slides, more in the backup

some comments on smoothing

- the implementation[21] I'm using has one user-defined parameter: the fraction of points used in the estimation
- after checking a few values I settled on 0.5 (default value is 0.6)
- the choice of the fraction mediates how much variance will be traded for bias
- for our purposes this treatment seems sufficient
- impact on branching fractions not very significant

branching fraction errors (%)

	$W \rightarrow e$	$W \rightarrow \mu$	$W \rightarrow \tau$	$W \rightarrow h$
no smoothing	0.92	0.69	1.83	0.4
smoothed	0.91	0.69	1.92	0.41

constraint on n.p. ($\sigma_{postfit}/\sigma_{prefit}$)

	ISR	FSR	ME-PS (hdamp)	UE/MPI (tune)
no smoothing	0.22	0.17	0.12	0.15
smoothed	0.27	0.08	0.11	0.19

[3] https://www.statsmodels.org/stable/generated/statsmodels.nonparametric.smoothers_lowess.lowess.html

Likelihood scans of JES n.p.

- carried out the scans of n.p. as before
- this is particularly useful for the JES:
  - accounting for values further from the central value, the "underconstraining" effect appears less severe
  - for example, the *absolute scale* n.p. constraint was 1.6 from the covariance matrix, but 1.1 from the scan
- complete set of scans here[22]

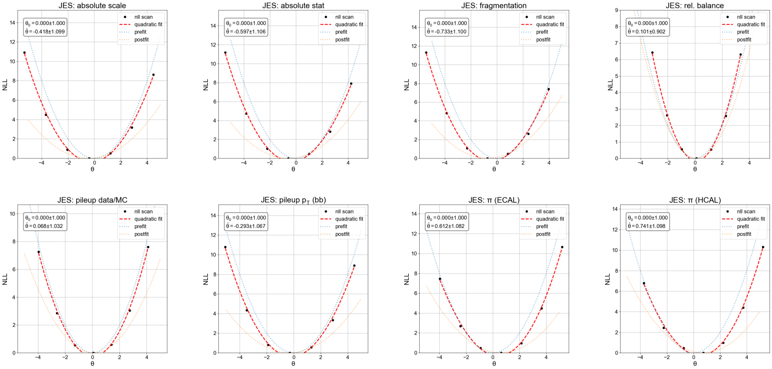

1 https://drive.google.com/open?id=1IDODhdYbzEEECLYI-dP-2QzERo_Jot_A

Investigating e+jet QCD estimate

- QCD is estimated using the fake rate method: select events with electrons failing isolation and apply fake rate factors
- same procedure as with muons where no issue is observed
- an ad hoc factor is applied to account for vetoing jets that overlap with the fake object
- visually, this background seems reasonable (see more plots here[23])

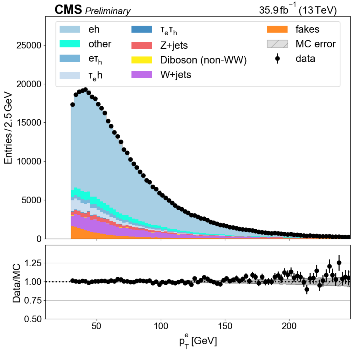

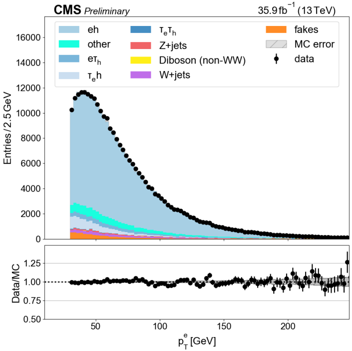

26 https://drive.google.com/open?id=1Us-AJ5Gydu-jS6XpTc-NJ-5w_3z9Pn3E

Investigating e+jet QCD estimate

- Ziheng has revisited the estimation of the fake rate transfer factors (in attached set of slides) using a $Z \to \mu\mu$+jet enriched region
- to make this consistent with the signal region, the requirement that the probe object be trigger matched was added
- this greatly increases the scale factors, and also significantly reduces the statistical precision of the estimate

$pT_{\tilde{l}}$	[15, 17)	[17, 20)	[20, 25)	[25, 30)	[30, 40)	[40, 50)
SF $\tilde{e}$	0.181+/-0.018	0.150+/-0.016	0.165+/-0.017	0.171+/-0.025	0.311+/-0.037	0.412+/-0.078
SF $\tilde{\mu}$	0.066+/-0.007	0.059+/-0.007	0.046+/-0.008	0.049+/-0.012	0.054+/-0.014	0.110+/-0.030

$pT_{\tilde{l}}$	[15, 17)	[17, 20)	[20, 25)	[25, 30)	[30, 40)	[40, 50)
SF $\tilde{e}$, pass trigger	-	-	-	-	2.1+/-0.6	2.8+/-1.0
SF $\tilde{\mu}$, pass trigger	-	-	-	1.8+/-1.1	1.00+/-0.46	3.1+/-1.4

Additional checks

- the effect of multiple fakeable electrons in the application region was checked $\to$ only $\approx 2\%$ of events have more than two objects
- fake rate in $\ell + \tau$ region checked

SF $j \to \tau$

SF $j \to \tau$ is measured from $ee + \tau_h$, $\mu\mu + \tau_h$ and $e\mu + \tau_h$ region. The sensitivity to $b \to \tau_h$ is dominated by $e\mu + \tau_h$ region enriched with leptonic $t\bar{t}$ plus $b \to \tau_h$.

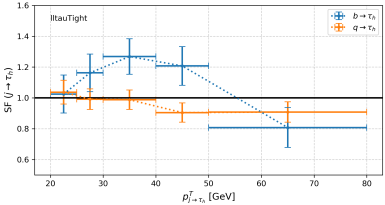

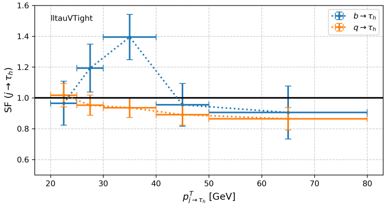

$p^T_{\tau_h}$ [GeV]	20-25	25-30	30-40	40-50	50-80
$SF(b \to \mathrm{Tight}\ \tau_\mathrm{h})$	1.02 ± 0.12	1.16 ± 0.12	1.27 ± 0.11	1.21 ± 0.13	0.81 ± 0.13
$SF(q \to \mathrm{Tight}\ \tau_\mathrm{h})$	1.04 ± 0.08	0.99 ± 0.07	0.99 ± 0.06	0.90 ± 0.06	0.91 ± 0.07
$SF(b \to \mathrm{VTight}\ \tau_\mathrm{h})$	0.97 ± 0.14	1.19 ± 0.16	1.39 ± 0.15	0.96 ± 0.14	0.91 ± 0.17
$SF(q \to \mathrm{VTight}\ \tau_\mathrm{h})$	1.02 ± 0.08	0.95 ± 0.07	0.94 ± 0.06	0.89 ± 0.07	0.86 ± 0.07

Table: $SF(j \to \tau_h)$ for Tight and VTight tau.

QCD in $l + jet$ channel

$\mathrm{SF}^{\overline{\mathrm{iso}}\to\mathrm{iso}}(\mathrm{pt}, \eta)$ is measured in $l + jet$ with

- $1 \leq n_j < 4, n_b \geq 1$
- $m^T_{l,met} < 40$ GeV

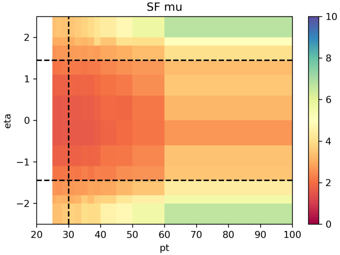

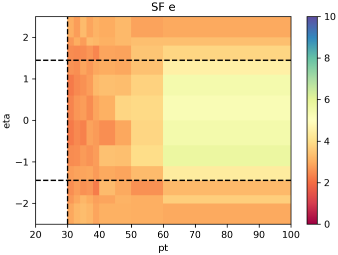

BSM

In B_W measurement, W mainly comes from the top decay. The popular BSMs that could lead to τ enhancement in the top decay include

- W' in the G221 nonuniversal gauge interaction model (NUGIM). The first two gen and the third gen fermions transform under two separate $SU(2)_{1,2}$ group with a mixing angle θ_E, which leads to nonuniversality. The $SU(2)_1 \times SU(2)_2$ breaks into the SM $SU(2)_L$ at low energy scale.
- H^+ in the 2HDM. Higgs sector has two scalar doublets with a mixing angle β. Charged higgs couples stronger to τ than e, μ due to tau's higher mass. Type-II is considered.
- leptoquark. If LQ conserves generation, the LQ from top tends to decay into tau. LQ is predicted by many GUT. But the interpretation with LQ is very model dependent.

Estimate MUGIM W' Exclusion

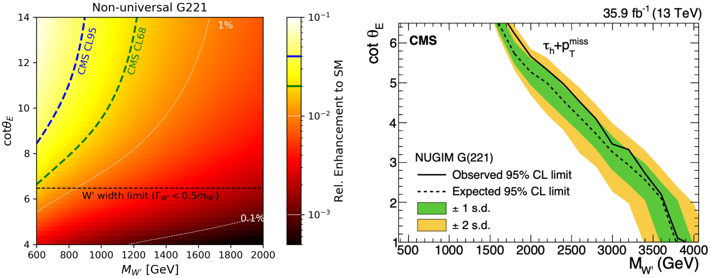

Figure: NUGIM: exclusion of ours (left) and the direct search[25](right) . Our result does not exclude more phase space than the direct search.

[25] 10.1016/j.physletb.2019.01.069

Estimate Type-II 2HDM Exclusion

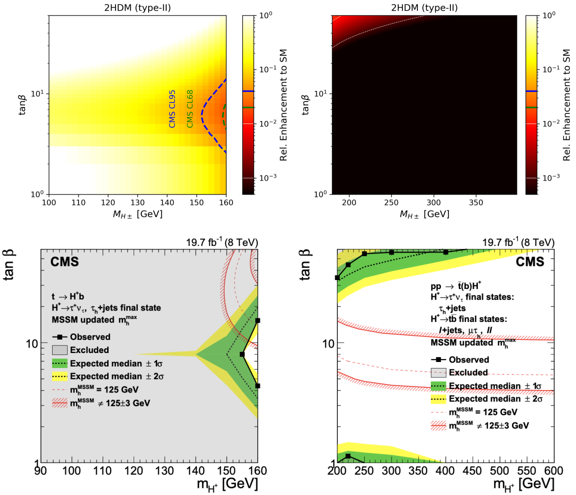

Figure: Type-II 2HDM: exclusion of ours (upper) and the direct search [27] (lower). Our result does not exclude more phase space than the direct search.

[27] 10.1007/JHEP11(2015)018

Yasmine Sara Amhis et al.
Averages of b-hadron, c-hadron, and τ-lepton properties as of 2018.
Eur. Phys. J. C, 81(3):226, 2021.

M. Huschle et al.
Measurement of the branching ratio of $\bar{B} \to D^{(*)}\tau^-\bar{\nu}_\tau$ relative to $\bar{B} \to D^{(*)}\ell^-\bar{\nu}_\ell$ decays with hadronic tagging at Belle.
Phys. Rev. D, 92(7):072014, 2015.

Y. Sato et al.
Measurement of the branching ratio of $\bar{B}^0 \to D^{*+}\tau^-\bar{\nu}_\tau$ relative to $\bar{B}^0 \to D^{*+}\ell^-\bar{\nu}_\ell$ decays with a semileptonic tagging method.
Phys. Rev. D, 94(7):072007, 2016.

S. Hirose et al.
Measurement of the τ lepton polarization and $R(D^*)$ in the decay $\bar{B} \to D^*\tau^-\bar{\nu}_\tau$.
Phys. Rev. Lett., 118(21):211801, 2017.

J.P. Lees et al.
Evidence for an excess of $\bar{B} \to D^{(*)}\tau^-\bar{\nu}_\tau$ decays.
Phys. Rev. Lett., 109:101802, 2012.

J.P. Lees et al.
Measurement of an Excess of $\bar{B} \to D^{(*)}\tau^-\bar{\nu}_\tau$ Decays and Implications for Charged Higgs Bosons.
Phys. Rev. D, 88(7):072012, 2013.

Roel Aaij et al.
Measurement of the ratio of branching fractions $\mathcal{B}(\bar{B}^0 \to D^{*+}\tau^-\bar{\nu}_\tau)/\mathcal{B}(\bar{B}^0 \to D^{*+}\mu^-\bar{\nu}_\mu)$.
Phys. Rev. Lett., 115(11):111803, 2015.
[Erratum: Phys.Rev.Lett. 115, 159901 (2015)].

R. Aaij et al.
Measurement of the ratio of the $B^0 \to D^{*-}\tau^+\nu_\tau$ and $B^0 \to D^{*-}\mu^+\nu_\mu$ branching fractions using three-prong τ-lepton decays.
Phys. Rev. Lett., 120(17):171802, 2018.

R. Aaij et al.
Test of Lepton Flavor Universality by the measurement of the $B^0 \to D^{*-}\tau^+\nu_\tau$ branching fraction using three-prong τ decays.
Phys. Rev. D, 97(7):072013, 2018.

C. Albajar et al.
Studies of Intermediate Vector Boson Production and Decay in UA1 at the CERN Proton - Antiproton Collider.
Z. Phys. C, 44:15–61, 1989.

JA Appel, P Bagnaia, M Banner, R Battiston, K Bernlöhr, K Borer, M Borghini, G Carboni, Vincenzo Cavasinni, P Cenci, et al.
Measurement of w$\pm$and z0 properties at the cern pp collider.
Zeitschrift für Physik C Particles and Fields, 30(1):1–22, 1986.

J. Alitti et al.
A Measurement of electron - tau universality from decays of intermediate vector bosons at the CERN anti-p p collider.
Z. Phys. C, 52:209–218, 1991.

J. Alitti et al.
A Search for charged Higgs from top quark decay at the CERN $\bar{p}p$ collider.
Phys. Lett. B, 280:137–145, 1992.

F. Abe et al.
A Measurement of $\sigma B(W \to e\nu)$ and $\sigma B(Z^0 \to e^+e-)$ in $\bar{p}p$ collisions at $\sqrt{s} = 1800$ GeV.
Phys. Rev. D, 44:29–52, 1991.

F. Abe et al.
A Measurement of the production and muonic decay rate of W and Z bosons in $p\bar{p}$ collisions at $\sqrt{s} = 1.8$ TeV.
Phys. Rev. Lett., 69:28–32, 1992.

F. Abe et al.
Measurement of the ratio $\sigma B(W \to \nu_\tau)/\sigma B(W \to e\nu)$, in $p\bar{p}$ collisions at $\sqrt{s} = 1.8$ TeV.
Phys. Rev. Lett., 68:3398–3402, 1992.

B. Abbott et al.
Extraction of the width of the W boson from measurements of $\sigma(p\bar{p} \to W + X) \times B(W \to e\nu)$ and $\sigma(p\bar{p} \to Z + X) \times B(Z \to ee)$ and their ratio.
Phys. Rev. D, 61:072001, 2000.

V.M. Abazov et al.
Combination of CDF and D0 Results on W Boson Mass and Width.
Phys. Rev. D, 70:092008, 2004.

S. Abachi et al.
W and Z boson production in $p\bar{p}$ collisions at $\sqrt{s} = 1.8$-TeV.
Phys. Rev. Lett., 75:1456–1461, 1995.

B. Abbott et al.
A measurement of the $W \to \tau\nu$ production cross section in $p\bar{p}$ collisions at $\sqrt{s} = 1.8$ TeV.
Phys. Rev. Lett., 84:5710–5715, 2000.

G. Abbiendi et al.
Measurement of the e+ e- —> W+ W- cross section and W decay branching fractions at LEP.
Eur. Phys. J. C, 52:767–785, 2007.

J. Abdallah et al.
Measurement of the W pair production cross-section and W branching ratios in e+ e- collisions at s**(1/2) = 161-GeV to 209-GeV.
Eur. Phys. J. C, 34:127–144, 2004.

P. Achard et al.
Measurement of the cross section of W-boson pair production at LEP.
Phys. Lett. B, 600:22–40, 2004.

A. Heister et al.
Measurement of W-pair production in e+ e- collisions at centre-of-mass energies from 183-GeV to 209-GeV.
Eur. Phys. J. C, 38:147–160, 2004.

S. Schael et al.
Electroweak Measurements in Electron-Positron Collisions at W-Boson-Pair Energies at LEP.
Phys. Rept., 532:119–244, 2013.

Ansgar Denner.

Techniques for calculation of electroweak radiative corrections at the one loop level and results for W physics at LEP-200.
Fortsch. Phys., 41:307, 1993.

Bernd A. Kniehl, Fantina Madricardo, and Matthias Steinhauser.

Gauge independent W boson partial decay widths.
Phys. Rev. D, 62:073010, 2000.

David d'Enterria and Matej Srebre.

α_s and $\mathrm{V_{cs}}$ determination, and CKM unitarity test, from W decays at NNLO.
Phys. Lett. B, 763:465, 2016.

Morad Aaboud et al.

Precision measurement and interpretation of inclusive W^+ , W^- and Z/γ^* production cross sections with the ATLAS detector.
Eur. Phys. J. C, 77(6):367, 2017.

Roel Aaij et al.

Measurement of forward W and Z boson production in pp collisions at $\sqrt{s} = 8$ TeV.
JHEP, 01:155, 2016.

Roel Aaij et al.

Measurement of forward $W \to e\nu$ production in pp collisions at $\sqrt{s} = 8$ TeV.
JHEP, 10:030, 2016.

Georges Aad et al.

Test of the universality of τ and μ lepton couplings in W-boson decays from $t\bar{t}$ events with the ATLAS detector.
7 2020.

A. Zupanc et al.

Measurements of branching fractions of leptonic and hadronic D_s^+ meson decays and extraction of the D_s^+ meson decay constant.
JHEP, 09:139, 2013.

J.P. Alexander et al.

Measurement of $B(D_s^+ \to e^+\nu)$ and the Decay Constant fD_s^+ From 600 $/pb^{-1}$ of $e^{\pm}$ Annihilation Data Near 4170 MeV.
Phys. Rev. D, 79:052001, 2009.

P.U.E. Onyisi et al.
Improved Measurement of Absolute Branching Fraction of D(s)+ —> tau+ nu(tau).
Phys. Rev. D, 79:052002, 2009.

P. Naik et al.
Measurement of the Pseudoscalar Decay Constant f(D(s)) Using D(s)+ —> tau+ nu, tau+ —> rho+ anti-nu Decays.
Phys. Rev. D, 80:112004, 2009.

P. del Amo Sanchez et al.
Measurement of the Absolute Branching Fractions for $D_s^- \to \ell^- \bar{\nu}_\ell$ and Extraction of the Decay Constant f_{D_s}.
Phys. Rev. D, 82:091103, 2010.
[Erratum: Phys.Rev.D 91, 019901 (2015)].

Medina Ablikim et al.
Measurement of the $D_s^+ \to \ell^+ \nu_\ell$ branching fractions and the decay constant $f_{D_s^+}$.
Phys. Rev. D, 94(7):072004, 2016.

Medina Ablikim et al.
Determination of the pseudoscalar decay constant $f_{D_s^+}$ via $D_s^+ \to \mu^+ \nu_\mu$.
Phys. Rev. Lett., 122(7):071802, 2019.

L. Widhalm et al.
Measurement of D0 —> pi l nu (Kl nu) Form Factors and Absolute Branching Fractions.
Phys. Rev. Lett., 97:061804, 2006.

D. Besson et al.
Improved measurements of D meson semileptonic decays to pi and K mesons.
Phys. Rev. D, 80:032005, 2009.

Bernard Aubert et al.
Measurement of the hadronic form-factor in $D^0 \to K^- e^+ \nu_e$ 1.
Phys. Rev. D, 76:052005, 2007.

M. Ablikim et al.
Study of Dynamics of $D^0 \to K^- e^+ \nu_e$ and $D^0 \to \pi^- e^+ \nu_e$ Decays.
Phys. Rev. D, 92(7):072012, 2015.

Medina Ablikim et al.
Study of the $D^0 \to K^- \mu^+ \nu_\mu$ dynamics and test of lepton flavor universality with $D^0 \to K^- \ell^+ \nu_\ell$ decays.
Phys. Rev. Lett., 122(1):011804, 2019.